NTNU
Norwegian University of
Science and Technology

Cooling of Buried Power Cables by Using Metallic Pipes as an Alternative to Polymeric Pipes

Comparison of Results from Experiments and Simulations

Tord Beck Sletten

Master of Science in Electric Power Engineering
Submission date: June 2016
Supervisor: Erling Ildstad, ELKRAFT

Norwegian University of Science and Technology
Department of Electric Power Engineering

NORGES TEKNISK-NATURVITENSKAPELIGE UNIVERSITET
NTNU

Hovedoppgave Våren 2016

Kandidatens navn:	Tord Beck Sletten
Fag:	Electric Power Engineering
Oppgavens tittel (norsk):	**Kjøling av nedgravde kraftkabler ved å bruke metalliske rør som et alternativ til plastrør.** Sammenlikning av resultater fra eksperimenter og simuleringer.
Oppgavens tittel (engelsk):	**Cooling of buried power cables by using metallic pipes as an alternative to polymeric pipes.** Comparison of results from experiments and simulations.

To day, the maximum current load capacity of buried power cables is rarely used. This is however about to change, as the society need of electric energy as well as short-term high current load capacity is increasing. Thus, improved knowledge about the thermal load characteristics and maximum current capacity of cable systems is becoming increasingly important, in order to avoid risk of premature deterioration and thermal damage of expensive cable installations.

This master project is a continuation of the project on Calculation of transient temperatures of buried cables, performed during the fall of 2015. The main purpose of the candidates MSc study is to use laboratory experiments and computer simulations to determine steady state temperature distributions in and around selected cable samples, directly buried in sand compared to metallic and polymeric pipes. The thesis is expected to constitute of:

- A literature survey, including theory, forming the base for suggested methods for thermal design of cable tracks.
- Description of working principle and limitations regarding thermal COMSOL simulations.
- Design of a laboratory experiment particularly aiming at testing the temperature of current loaded cables buried directly in sand, in PVC- and aluminum pipes.

- Results from measurements of material parameters and relevant results from COMSOL simulations, comparable with the experimental setup.
- Compare and evaluate the measured and simulated results.
- Discussion of the validity regarding the used approach, and suggestions for further work.

The details of the test program are to be decided in cooperation with the supervisor.

Start:	18 januar 2016
Innlevering:	17 juni 2016
Faglærer:	Professor Erling Ilstad (Erling.Ildstad@elkraft.ntnu.no)

Acknowledgement

This thesis terminates my master's degree within Electric Power Engineering at the Norwegian University of Science and Technology. There is no doubt that these years have been the most rewarding time of my life, but unfortunately, the time has come to an end. It definitely hurts me to say that I will not be a student any more. However, the production of this thesis has been quite demanding and stressful. My every intention was to provide you with interesting reading, and I hope that that I succeeded in that.

This was for sure not a one-man show. I would explicitly like to thank my supervisor, professor Erling Ildstad, for guiding me through this thesis from start to finish. It was very challenging at times, but with your expertise, everything turned out just fine. We had many great discussions, and we were always on the same page. I am very grateful for all the time you invested in me.

A good social environment is invaluable, and I would like to thank all my classmates throughout these years, and for all the good times we shared together. We might get separated now, but the good times will never be forgotten, nor will you. I would also like to thank my parents for supporting me from day one by saying "You can do this!". They were right on that. A special thanks goes to my brother, Sondre, for giving be guidance on my English when I needed it. I would also like to thank Hans Sæternes at Sintef for providing me with thermal conductivity measurements. A special thanks to Bård at the laboratory and Morten at Sintef's work shop for all help and practical contributions.

At last, my biggest gratitude goes out to the person who is currently carrying my first, unborn child. Kine Lovise, I can say for sure that this master thesis would never existed if it wasn't for you. Without you, I'm nothing. Thank you for believing in me, trusting me and caring for me. You are my rock, and I can not wait having our daughter together.

Thank you

Tord Beck Sletten
June 2016, Trondheim

Abstract

It is common to install power cables in polymeric pipes at road crossings and in urban areas where exceptional protection and flexibility is necessary. In such case, the pipe is usually filled with air, which increases the thermal resistance to the ambient surroundings, thus leading to a higher conductor temperature compared to if the cable was installed directly in soil. As a consequence, the current carrying capacity of the cable is limited by the high temperature inside the pipe, leading to a poor utilization of the cable.

This thesis has emphasized whether a metallic pipe can lower the operating conductor temperature of a power cable when compared to a polymeric pipe, due to the low thermal resistance of metals. To investigate this hypotheses, a laboratory experiment was conducted with a duration of approximately 3 months. Three different models were constructed, each with its own design of cable installation. These included direct burial in soil, installation in a buried polymeric pipe and installation in a buried aluminum pipe. A three phase cable was installed in series through each model, which was energized with three variac-controlled transformers. In addition, the experiment was simulated by the help of finite element software, and both results were analysed and compared to each other.

The main finding from the experiment was a lower conductor temperature inside the aluminum pipe compared to the polymeric pipe, and that the lowest operating temperature solely occurred in direct installation in soil. The simulations suggested a much higher temperature deviation between the two pipes compared to the results from the experiment. It was found that the models were too short, leading to a large amount of longitudinal heat transportation which was difficult to analytically compensate for in the simulations. Despite deviations between the experiment and simulations, aluminum pipes seems to have a great potential regarding natural cooling of cables, thus increasing the cables current carrying capacity.

Keywords: Experiment, aluminum pipe, PVC pipe, FEM.

Sammendrag

Det er normalt å forlegge kraftkabler i plastrør ved vegkryssinger og i urbane strøk hvor det stilles krav til ekstra beskyttelse og fleksibilitet. I slike tilfeller er røret ofte fylt med luft, noe som øker den termiske motstanden og deretter ledertemperaturen, sammenliknet med å legge kabelen rett i jorda. Konsekvensen er at strømføringsevnen til kabelen blir begrenset av temperaturen inne i røret, noe som er en dårlig utnyttelse av kabelen.

I denne oppgaven har det blitt lagt vekt på om metalliske rør kan senke ledertemperaturen sammenliknet med plastrør med tanke på den lave termiske motstanden i metall. For å undersøke denne hypotesen har det vært utført et eksperiment med en varighet av tre måneder. Tre forskjellige modeller ble bygd, hvor hver av dem representerte én forlegningsmetode. Disse forlegningsmetodene inkluderte direkte forlegning i jord, forlegning i et nedgravd aluminiumsrør og forlegning i et nedgravd plastrør. En trefasekabel ble forlagt i serie gjennom modellene, og kabelen ble spenningsatt ved hjelp av tre variac-styrte transformatorer. I tillegg ble resultatene fra eksperimentet sammenliknet med simuleringer fra et finite element-dataprogram.

Hovedfunnet er at ledertemperaturen inne i aluminiumsrøret var lavere sammenliknet med plastrøret. Den laveste ledertemperaturen var utelukkende målt i direkte forlegning i jord. Simuleringene antydet et mye større avvik i temperatur mellom plast- og aluminiumsrøret sammenliknet med resultatene fra eksperimentet. Det ble oppdaget at modellene var for korte, og at mye varme fra kabelen forsvant i lengderetning av modellene. Dette varmetapet var vanskelig å kompensere mot rent analytisk i simuleringene. Til tross for avvikene mellom eksperimentet og simuleringene ble det funnet et stort potensial for å bruke aluminiumsrør til naturlig nedkjøling av kablene, noe som kan føre til høyere strømføringsevne for kablene.

Nøkkelord: Eksperiment, aluminiumsrør, PVC-rør, FEM.

Contents

List of Figures

List of Tables

Chapter 1

Introductory Information

1.1 Introduction

For most electric installations, it is common consensus that the operating temperature is the most dominating factor for reduced lifetime of the installation. If the operating temperature exceeds the recommended value, the installation in hand can suffer from a premature breakdown. High voltage underground power cables are not an exception. The consequences of thermal and electrical breakdown in power cables are obvious; down time in power supply, economical losses and human safety to name a few. In the upcoming future, the consequences of a breakdown can possibly be even higher than for today, due to increasing need of electric energy. It is therefore crucial for electrical engineers to know why, when and where a power cables is overloaded, as well as developing new knowledge on the topic.

A cables ampacity[1] is often calculated based on the location in which the highest temperature occurs. As an example, if an underground power cable is installed inside a plastic pipe, a higher conductor temperature will occur compared to the same cable installed directly in soil. Installations in pipes are unfortunately inevitable in many situations, such as road crossings. It is therefore of interest to examine if the pipe-design can be improved, hence provide the cable with a more effective and natural cooling, without increasing the complexity of the design. An idea came to mind while considering this problem, which was to replace the plastic pipe with a metallic pipe. The hypothesis was that metal could transport the heat loss away from the cable more efficient than plastics, due to the beneficial thermal properties of metals. To reveal the validity of this hypotheses, an experiment was constructed and executed with three different installation designs. These included cable installation inside a buried polymer pipe and direct installation in soil. The third design included installation inside a buried aluminum pipe. Prior to the experiment, no literature was found regarding thermal performance of power cables inside aluminum

[1] Ampacity is an expression of a cables current carrying capacity.

pipes, which makes this experiment unique.

This thesis presents the complete work of the experiment, including relevant theory, choice of method, execution of the experiment, results and a thorough discussion. It was found that the aluminum pipe can reduce the operating temperature of the cable when compared to a polymeric pipe. The reduction in temperature was, however, much lower than simulated on the computer. Parts of this deviation was revealed by the help of analytical approximations, whereas the remained deviation was due to uncertainty factors. In addition, the lowermost operating temperature was observed in direct installation in soil, regardless of the applied current.

1.2 Subject of Interest and Scope of Work

In [8], several designs of underground cable plants were analysed. It was concluded that the presence of an aluminum pipe in an underground power cable system can increase the ampacity of the cable when compared to a traditional plastic pipe. The main reason for this finding was the fact that aluminum conducts heat very well compared to plastic pipes made of polyvinyl-chloride (PVC) or polypropylene (PP). However, since the finding was based on computer simulations, the trustworthiness of the conclusion was limited to a that extend: simulation- and analytically based only. To reveal whether aluminum is a better choice than polymers, it was chosen to construct and execute an experiment at the high current-laboratory at NTNU.
The scope of the experiment was limited based on the accessibility of materials, equipment and of course time limitations. To exploit the possibilities, it was chosen to build models of the three cable plants, instead of constructing full scale systems. Subsequently, the cables in use was arbitrary chosen as 3 x 25 mm^2 single phased XLPE insulated cables, with a total length of about 15 metres. The main attention was paid to the differences in temperature performance between the different designs. Much attention was also paid to the construction of the experiment itself, and assessment of its validity. No attention was paid to the ampacity of the cable, but rather on how the temperature evolved in each design, and to the reason for the different temperatures. To obtain the desired data, three separate experiments were conducted with arbitrary applied currents. Furthermore, to study the correlation between the obtained results and analytical computations, COMSOL[2] was used as a reference. The objective of using FEM-software in combination to the experiment was to strengthen the discussion regarding the validity of the experiment, and to reveal possible deviations.

[2]COMSOL is a finite element (FEM) software used for simulations.

1.2.1 Thesis Overview

This master thesis is separated into three main parts, excluding the first chapter:

- **Theory** which contains the needed theory to understand the obtained results and the discussion from the experiment and the simulations.
- **Experiments and Data Collection** which covers the method used regarding construction and conduction of the experiment. Detailed information is being presented in order to make the experiment reconstructible. The results are presented in this part, both from the experiment and the simulations.
- **Discussion and Conclusion** which holds thorough discussion of the obtained results from the experiments and the simulations. Finally comes the conclusion and a recommendation for future work within the same topic.

1.2.2 Master Thesis Formalities

This report is a master thesis which terminates the authors education of five years. The study programme is named Master of Science in Electric Power Engineering at the Norwegian University of Science & Technology (NTNU). All of the work resulting in this thesis was performed during the spring of 2016, and the thesis accounts for 30 credits.
The organization of this work is collaborated between the author of this thesis and his supervisor, professor Erling Ilstad at the Department of Electric Power Engineering. The experiment was performed at the heat-current laboratory at NTNU. No other organizations or companies had any direct influence on the experiment in any way. Anyone is free to use this thesis as a reference to his or hers own work.

1.2.3 Problem Formulation and Goals

The purpose of this thesis is to construct and execute a laboratory experiment to collect quantitative data for comparison of three different designs of underground power cable systems. The primary goal of this work is to find out if a cable installed inside a buried aluminum pipe can decrease the conductor temperature, when compared to a PVC pipe. The secondary goal is to assess the validity of the experiment by comparing the results to simulations in COMSOL, and to assess any observed deviations by the help of analytical procedures.

Part I

Theory

Chapter 2

A Review of Literature

This part contains relevant theory which is used as a base for the actions in Part II and the discussions in Part III.

2.1 Categories

For this thesis, the literature of interest is divided into four topics. The first includes the use of COMSOL. This programme was used as a second comparison to the laboratory experiment. Secondly comes literature regarding design of underground power systems and ampacity calculations. Third comes the use of aluminum pipes as a design criteria for underground power cables, and the corresponding loss calculations. Finally comes the practical aspect of conducting an experiment where cables are to be energized, as done in this thesis. In addition is [8] of high relevance, since it was a preliminary study to this thesis performed by the author.

2.1.1 Finite Element Analysis

The use of finite element programs (FEM) has become inevitable the last decades within many fields of science. The concept is based on numerical methods within a given mesh of a given geometry. All kinds of geometries can be drawn, and the equations are build-in to the chosen physics, such as Maxwell‘s equations in the electrostatic and electromagnetic environment. In this thesis, COMSOL was chosen as a solution to FEM. Several user‘s guide can be found such as [14]. More information about COMSOL is being presented in chapter 5.

2.1.2 Design Of Underground Power Cable Systems

Regarding design of underground power cable systems, the most complete work can be found in [1]. The author of this book, professor George J. Anders, is considered as one of the most competent scientists within the field today. He has written and contributed

to several books and papers such as [1], [2], [3], [10] and more. The work of Anders can be considered as highly trustworthy. When performing analytical ampacity calculations, [1] contains all needed theory to conduct most calculations and problems. In addition, [4] contains much information regarding typical designs of underground power cable systems. It also provides ampacity tables for most types of designs which is common today, such as installation of cables in ducts, pipes, on cable ladders etc, conduits etc. Nexans claims that direct burial of cables are widely used all over the world. When cables are directly buried, they are usually installed flat or in a trefoil formation with a minimum excavation depth of 70 cm. When cables are to cross roads, they are often placed in polymeric pipes surrounded by concrete, which is preferred for cables above 225 kV. However, [4] do not provide any information regarding cable installation in metallic pipes such as aluminum.

2.1.3 Hysteresis And Eddy Current Losses in Metallic Pipes

The encountered problems with placing cables in metallic pipes, are eddy current- and hysteresis losses. In [12], losses in steel pipes were considered. In this case, a current carrying tube was placed in the center of a steel pipe. Both hysteresis and eddy current losses were examined. It was found that hysteresis losses can triple the total losses in the pipe in comparison to eddy currents only. This is because of the high, non-linear permeability of steel. It was also found that the hysteresis itself alter the eddy currents, meaning that the eddy currents will be higher than necessary. A similar paper [10] presents an advanced analysis of losses in steel pipes with cables placed inside the pipes at different geometrical locations. The authors (including Anders) also took consideration to screen losses. Among several observations, they found a great share of hysteresis loss in the pipes.

In [13], different theoretical calculations regarding losses in pipes were examined. A comparative experimental study was performed to compare empirical data versus calculated data. Among many findings, they found that the thickness of the pipe, both aluminum and steel, plays a role regarding eddy current losses. The loss (W/m) stabilized when the ratio between thickness and skin depth[1] was greater than one. They also found that a flat formation in metallic pipes will create higher losses in the pipes compared to a trefoil formation. As far as understood by the author of this thesis, they did not include hysteresis losses in this particular paper. They did, however, present a useful technique regarding loss measurements in metallic pipes. To sum up, pipes made of high permeability materials seems to be unfavourable due to hysteresis loss. It was therefore chosen to use an aluminum pipe for this experiment because aluminum in a non-magnetic material, hence no hysteresis will occur.

[1]Skin depth is the depth of a conductor where the current density, J, has dropped to a value of 1/e compared to the surface density. This is due to the skin effect caused by alternating currents [11].

2.1.4 Experimental Study And Practical Aspects

Regarding practical performance of a laboratory experiment as the one in this thesis, [7] is a very good and informative paper. The authors constructed a full size model of a cable system and energized the cable with 300 A and 600 A for 570 and 230 hours, respectively. The construction technique they used for the experiment was used as an initial reference to the experiment in this thesis.

Chapter 3

The Basic Theory

3.1 A Review on Ampacity Calculations

This thesis is based on empirical research, but it is highly important to understand the basic, underlying theory behind the findings in these experiments. A short review on ampacity computations is hereby presented in such a way that the reader can revise his or hers knowledge on the field. If needed, further reading on the topic can be found in [8], [2] and [1] which are the main reference to the theory in the upcoming sections. Throughout this section, dielectric- and circulation losses are neglected.

When a current is applied to a cable, it is known that the the conductor temperature will rise due to molecule excitation. The heat produced by the conductor is then transferred to the ambient surroundings. The transport of heat will happen in one- or a combination of the following mechanisms:

- Convection
- Conduction
- Radiation

For a cable buried directly in soil, the main thermodynamics of matter is conduction, both internally in the cable and in the surrounding medium. This occurs when a molecule with high kinetic energy transmits some of its energy to another molecule with lower kinetic energy. Conduction dominates in solid substances, and can be expressed as:

$$P_{conduction} = \frac{A}{\rho_{th}} \frac{\partial \Theta}{\partial l} \tag{3.1}$$

In which:

$P_{conduction}$	is the conductive heat transfer (W)
A	is the effective area of heat flow
ρ_{th}	is the thermal resistivity of the material (m·K/W)
$\frac{\partial \Theta}{\partial l}$	is the temperature gradient in the body (K/m)

Convection occurs in gases, either in forced- or natural form, by means of mass transportation. Regardless of the form, the convection state holds a similarity to conduction. The exception is the *convection heat transfer coefficient*, h (W/m^2), which is proportional to heat transfer in the following equation:

$$P_{convection} = hA(\Theta_s - \Theta_a) \tag{3.2}$$

Where Θ_s and Θ_a is the surface- and ambient temperature, respectively.
The emitted heat transfer at the surface of a body, such as a cable installed in air, is called radiation. For a cable, the radiative heat transfer is given as:

$$P_{radiation} = \epsilon \sigma_B A_c(\Theta_s^4 - \Theta_a^4) \tag{3.3}$$

Where:

$P_{radiation}$	is the emitted heat transfer (W)
ϵ	is the emissivity at the surface of the body
σ_B	is the *Stefan-Boltzmann constant* ($5.64 \cdot 10^{-8}$ (W/m^2·K^4))

If present, the total heat rate is often expressed as the sum of these mechanisms. When calculating the ampacity of a cable, however, simplifications are often made to ease the calculations. This is done by rearranging equation 3.1 in the following way:

$$\Delta\Theta = \Theta_c - \Theta_a = P \cdot T \tag{3.4}$$

Where:

Θ_c	is the conductor temperature (K)
Θ_a	is the ambient temperature (K)
P	is the heat loss in the conductor (W)
T	is the thermal resistance (W/m·K) in the body between Θ_c and Θ_a

In physics, thermal resistance is known as a materials ability to impede heat. It has an unmistakable analogy to electric resistance, so equation 3.4 is in many ways based on electrical-thermal analogy. Thermal resistance can be a comprehensive task to obtain, but it is highly important due to the termination of the highest permissible current in a cable. The current can be determined based on the following equation ([1] chapter 4),

which is an expansion of 3.4:

$$I = \sqrt{\frac{\Delta\Theta}{R(T_1 + nT_2 + n(T_3 + T_4))}} \tag{3.5}$$

Where:

I	is the current (A)
$\Delta\Theta$	is the difference between the ambient- and conductor temperature (K)
R_{ac}	is the AC resistance of the conductor (Ω)
n	is the number of live conductors in the cable
T_1	is the thermal resistance between one conductor and the sheath (W/m·K)
T_2	is the thermal resistance in the bedding between the sheath and armour (W/m·K)
T_3	is the thermal resistance of the external serving of the cable (W/m·K)
T_4	is the thermal resistance of the surrounding medium (W/m·K)

The most dominating thermal resistance is often T_4, which holds the thermal resistance of a pipe (if present) and the surrounding soil. The impact of a pipe is discussed in the upcoming subsection.

3.1.1 The Impact Of A Pipe In Cable Laying Design

The external thermal resistance for a cable system including the presence of a pipe is according to [1]:

$$T_4 = T‘_4 + T“_4 + T“‘_4 \tag{3.6}$$

In which:

$T‘_4$	is the thermal resistance of the air between the conductors and the pipe
$T“_4$	is the thermal resistance of the pipe
$T“‘_4$	is the external thermal resistance of the pipe

The produced heat from the conductors is forced through T_4 towards the ambient surroundings. According to the previous discussion, the heat is transferred by conduction, convection and radiation to the ambient environment. Thus, an *energy balance equation* can be determined as:

$$P_c = P_{convection} + P_{conduction} + P_{radiation} \tag{3.7}$$

Where P_c is the heat loss from the conductors. P_c can be solved with respect to $T‘_4$:

$$T‘_4 = \frac{\Theta_s - \Theta_w}{P_c} = \frac{\Theta_s - \Theta_w}{P_{convection} + P_{conduction} + P_{radiation}} \tag{3.8}$$

Where Θ_s and Θ_w is the temperature at the cable surface and the wall of the pipe,

respectively. The computations for these parameters are quite complex. According to the author of [1], they are not suitable for standardization, and that the properties of the heat transfer equations are temperature dependant. Throughout this thesis, it has not been attempted to calculate these values for the given experiment. They are instead represented as a percentage distribution of the total thermal resistance in each of the three models, which is calculated in III based on the obtained results from the experiments. However, the thermal resistance of a metal pipe can be neglected compared to a PVC pipe. This fact is the main basis for the hypothesis that the presence of a non-magnetic metal pipe, such as aluminum, can lower the operating temperature of a cable with a given current, when compared to a PVC pipe.

3.2 Resistance Calculation

The objective of calculating the resistance of the cables used in this experiment, is to use it for heat loss calculations. Theses calculations are to be compared to the heat loss in the aluminum pipe, caused by induced eddy currents. In this way, one can assess the relative share of heat loss caused by eddy currents, and by the load current.

The resistance in a conductor increases when an alternating current is applied, compared to DC. This is due to eddy currents and the proximity effect. The cables used for the experiment where three 25 mm^2 conductors, insulated with a 3 mm thick layer of XLPE. All constants which is used to calculate AC resistance in this section are found in the international standard IEC 60287-1-1 [15]. For DC, the resistance of a conductor including temperature dependency is given as:

$$R_{DC} = \rho \frac{l}{A}(1 + \alpha(\Theta_c - 20\,^\circ\mathrm{C})) \tag{3.9}$$

In which:

- R_{DC} is the DC resistance of the conductor (Ω)
- ρ is the resistivity of the material ($2.82 \cdot 10^{-8}\Omega m$) for aluminum
- l is the length of the conductor (m)
- A is the cross section of the the conductor (m^2)
- α is the temperature coefficient for the material ($4.03 \cdot 10^{-3}(1/^\circ\mathrm{C})$
- Θ_c is the actual temperature in the conductor ($(1/^\circ\mathrm{C})$)

When the heat loss measurements in the pipe took place (subsection 6.5.1), the conductor temperature, Θ_c, was approximately 20 °C. For a 25 mm^2 aluminum conductor, the DC

resistance becomes:

$$R_{DC} = 2.82 \cdot 10^{-8} \frac{1}{25 \cdot 10^{-6}} = 1.128 \cdot 10^{-3} \Omega/m \tag{3.10}$$

The increase in resistance due to skin- and proximity effect can be written as:

$$R_{AC} = R_{DC}(1 + \gamma_s + \gamma_p) \tag{3.11}$$

In which:

R_{AC}	is the effective AC resistance when the conductor is applied with AC (Ω)
R_{DC}	is the DC resistance of the conductor (Ω)
γ_s	is the skin effect factor caused by eddy currents in the conductor
γ_p	is the proximity effect factor

Both the skin- and proximity effect factors are based on empirical equations. The skin effect factor is given as:

$$\begin{aligned} \gamma_s &= \frac{x_s^4}{192 + 0.8x_s^4} \\ x_s^2 &= \frac{8\pi f}{R_{DC}} 10^{-7} \cdot k_s \end{aligned} \tag{3.12}$$

In which:

f	is the supplied frequency (Hz)
k_s	is a constant which is found in [15] (1 for this purpose)

So the skin effect factor becomes:

$$\begin{aligned} x_s^2 &= \frac{8\pi 50}{1.128 \cdot 10^{-3}} 10^{-7} = 0.111 \\ \gamma_s &= \frac{0.111^2}{192 + 0.8 \cdot 0.111^2} = 6.41 \cdot 10^{-5} \end{aligned} \tag{3.13}$$

The proximity factor is a bit more complex. It is dependent on geometrical factors, frequency and cable type. Throughout this thesis, the attention is paid to single core cables, assembled in a trefoil configuration. The equation is given as:

$$\begin{aligned} \gamma_p &= \frac{x_p^4}{192 + 0.8x_p^4} (\frac{d_c}{s})^2 [0.312(\frac{d_c}{s})^2 + \frac{1.18}{\frac{x_p^4}{192+0.8x_p^4} + 0.27}] \\ x_p^2 &= \frac{8\pi f}{R_{DC}} 10^{-7} k_p \end{aligned} \tag{3.14}$$

In which:

f	is the supplied frequency (Hz)
k_p	is a constant found in [15] (1 for this purpose)
d_c	is the conductor diameter (mm)
s	is the distance between the conductor axes (mm)

By inserting the given numbers, the proximity effect becomes:

$$\begin{aligned} x_p^2 =& \frac{8\pi 50}{1.128 \cdot 10^{-3}} 10^{-7} = 0.111 \\ \gamma_p =& \frac{0.111^2}{192 + 0.8/cdot0.111^2} (\frac{5.64}{6})^2 [0.312 (\frac{5.64}{6})^2 + \frac{1.18}{\frac{0.111^2}{192+0.8 \cdot 0.111^2} + 0.27}] = 2.5 \cdot 10^{-4} \end{aligned} \tag{3.15}$$

Finally, the AC resistance of the conductors becomes:

$$R_{AC} = R_{DC}(1 + \gamma_s + \gamma_p) = 1.128 \cdot (1 + 6.41 \cdot 10^{-5} + 2.5 \cdot 10^{-4}) = 1.1283 \cdot 10^{-3} \Omega/m \tag{3.16}$$

In can therefore be concluded that the skin- and proximity factor are negligible for this particular configuration.

3.3 Monitoring and Assessment of Temperatures

It is obviously of great importance that the temperature measurements are as correct as possible. When temperature data is collected, one can calculate the temperature gradient at different locations, which can be used for calculation of heat transport. Due to the high thermal conductivity in the conductors, and the expected temperature differences between the models, it can be expected gradients in the longitudinal direction. The gradient in the z-direction (along the conductor) is defined as:

$$\nabla \theta_z = \frac{\partial \theta}{\partial_z} \tag{3.17}$$

This leads to the disadvantage of small models, which is the risk of *end effects* where the cables enters or leaves the box. This phenomena means that the temperature drops or increases gradually in the transition between the cable plant (the model) and outside of the plant. End effects are therefore monitored by the help of thermocouple probes both inside and outside of the models, as explained in section 6.4. A representation of this phenomena is being presented in Figure 3.3. The representation is self drawn, and it is not related to any real temperature measurements or calculations.

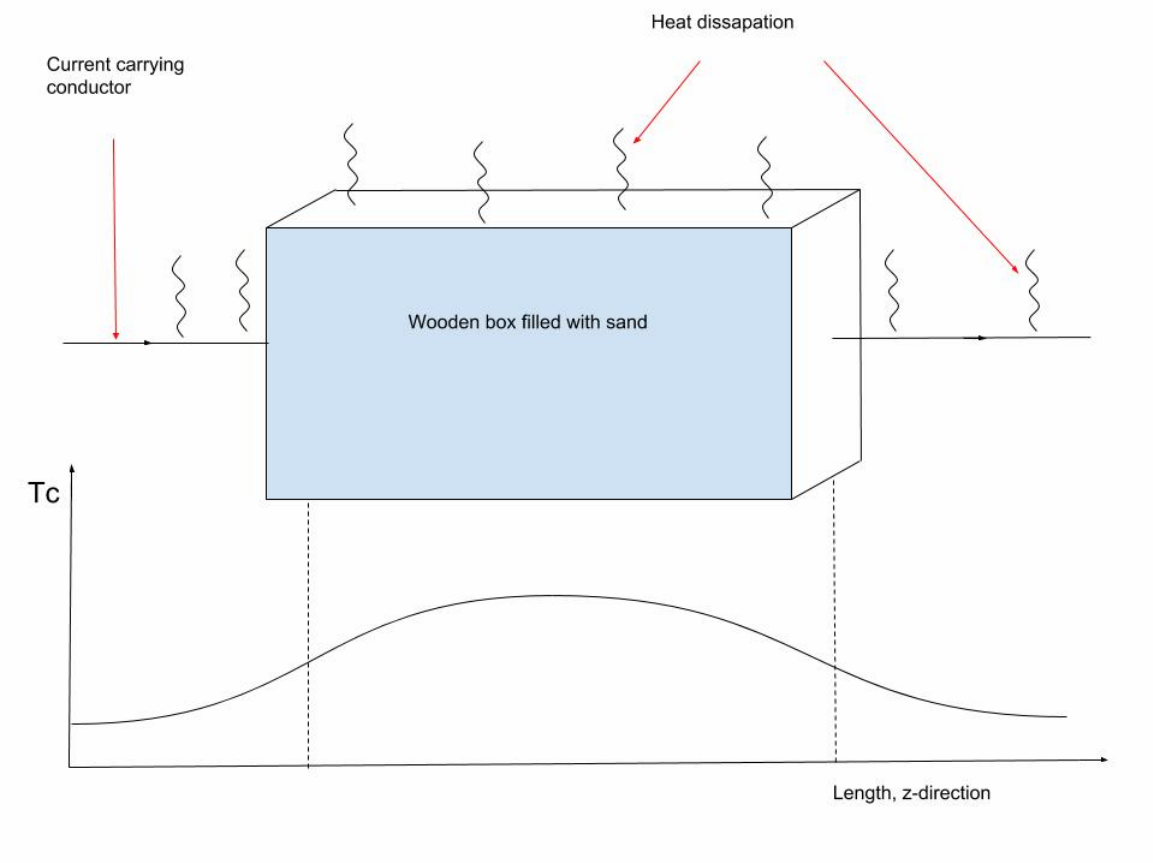

Figure 3.1: A plausible temperature gradient in the z-direction of the cables

3.4 Preparation For Specific Heat Measurements

The soils heat capacity is by far the most dominant for this experiment, considering the mass of the soil in comparison to the pipes and the cables. Knowing the specific heat capacity is a required parameter when conducting simulations in COMSOL, and it was therefore required to measure it by the help of a minor experiment. The upcoming theory was used to conduct the experiment, which is presented in 7.2.

If two solid materials with different temperatures are blended together, there will be heat transfer from the warmest material to the coldest in terms of conduction. Simultaneously, one can say that all extracted heat from the warmest material must be absorbed by the coldest material, given the condition of an adiabatic process. In other words, the heat absorbed by one material, is the lost heat from the second material. This is given as:

$$Q_1 = -Q_2 \tag{3.18}$$

Where Q_1 and Q_2 is the energy (J) in material 1 and 2, respectively. Q can in general be

written as:

$$Q = m \cdot c \cdot (\Theta_{final} - \Theta_{initial}) \tag{3.19}$$

In which:

m	is the mass of the material (kg)
c	the specific heat of the material (J/kg·K)
Θ_{final}	is the final temperature in the material (K)
$\Theta_{initial}$	is the initial temperature in the material (K)

In equation 3.18, $-Q_2$ implies that the temperature in material 2 drops from one temperature to another. Q_2 can therefore be written as:

$$-Q_2 = m_2 \cdot c_2 \cdot (\Theta_{final} - \Theta_{initial(2)}) = m_2 \cdot c_2 \cdot \Delta\Theta_2 \tag{3.20}$$

Since material 1 absorbs just as much energy as the energy lost in material 2, the equation becomes:

$$Q_1 = \mid -Q_2 \mid = m_1 \cdot c_1 \cdot (\Theta_{final} - \Theta_{initial(1)}) = m_1 \cdot c_1 \cdot \Delta\Theta_1 \tag{3.21}$$

Please remark the absolute value. This applies because material 1 absorbs energy, hence the plus-sign must be valid. Equation 3.18 can finally be solved with respect to the only unknown parameter, namely the specific heat capacity in material 1:

$$c_1 = \frac{m_2 \cdot c_2 \cdot \Delta\Theta_2}{m_1 \cdot \Delta\Theta_1} \tag{3.22}$$

Chapter 4

Electromagnetic Theory With Emphasis on Eddy Currents and Losses

In [8], it was concluded that an aluminum pipe has a great potential regarding increased ampacity for underground power cables. A drawback of the used methodology, was that the conductors were modelled as a heat source only. This means that the conductors were sat to produce a certain amount of heat (W) at a given time. No real currents were actually present in the cables, theoretically speaking. This also means that no magnetic fields excised. If a rotating magnetic field penetrates an object, there will an induced voltage in the object according to Faraday‘s Law. This voltage will in turn give rise to a current which subsequently generates a heat loss.
In this thesis however, eddy current losses are taken into consideration. Regarding this experiment, the main question is how large the losses are with respect to the conductor losses. If large losses are present, they will not only represent economical losses for the power utility, but they will also represent a heat source. To get an overview, background theory regarding this subject is being presented in the upcoming sections.

4.1 Induced Eddy Currents In The Pipe

A current carrying conductor will always generate a magnetic field. To increase the understanding of how the field is distributed in the x y-plane, one must take into consideration Amperes law of magnetic fields. For a conductor, Amperes law can be written as[11]:

$$\oint \overrightarrow{H}(t)dl = i_c(t) = I\sqrt{2}sin(\omega t) \tag{4.1}$$

In which:

$\overrightarrow{H}$	is the magnetic field strength (A/m)
I	is the RMS-value of the current
ω	is $2\pi f$
f	is the applied frequency (Hz)

The line integral of this equation says that the numerical sum of all components of the magnetic field must be numerically equal to the current that flows inside that path. This applies everywhere, both inside the conductor, at its surface and outside of the conductor. It can therefore be proved that the magnetic field strength will decrease at a $1/x$ rate away from the conductor. For a circular conductor, the line integral becomes:

$$\oint \overrightarrow{H} dl = 2\pi x \cdot H = i_c(x) \tag{4.2}$$

Where x is a variable distance from the center of the conductor, analytically speaking. At the same time, we know that the current is spread over the total area of the conductor. Most of it will appear close to the surface due to the skin effect[1]. The current enclosed inside that area will therefore be be a function of x:

$$i_c(x) = i_c \frac{\pi x^2}{\pi r^2} = i_c (\frac{x}{r})^2 \tag{4.3}$$

Where x can not exceed r. So, with x as a variable, Amperes law can be solved with respect to H:

$$H(x) = \frac{i_c}{2\pi r^2} x = i_c k \cdot x \tag{4.4}$$

In other words, the magnetic field strength increases proportionally to the distance from the center of the conductor, with a peak at the surface, as shown in Figure 4.1. When analysing the magnetic field outside the conductor, the field strength becomes:

$$H(x) = \frac{i_c}{2\pi x} \tag{4.5}$$

At $x > r$. This means that the magnetic field strength, hence the magnetic field density decreases at a $1/x$ rate away from the conductor. I also implies that the induced current in the pipe will decrease inversely to the distance from the conductor. Equation 4.5 is written with respect to *one* current. For a three phases system, the vectorial sum of balanced currents will always be zero:

$$i_a(t) + i_b(t) + i_c(t) = \sqrt{2} I e^{j\omega t} + \sqrt{2} I e^{j(\omega t - 2\pi/3)} + \sqrt{2} I e^{j(\omega t - 4\pi/3)} = 0 \tag{4.6}$$

[1]The skin effect is caused by induced eddy currents in the conductor due to the alternating magnetic field, caused by the main conductor current [11].

Which implies that the vectorial sum of the magnetic field strength, hence the magnetic flux density is zero:

$$H_a(t) + H_b(t) + H_c(t) = 0 \tag{4.7}$$

Based on geometrical factors of the conductors in the pipe, however, some of the magnetic field lines will be stronger than others inside the pipe itself. For example, the field strength produced by the uppermost conductor in a trefoil at the bottom of a pipe, will not be as strong inside the pipe compared to the field strength from the lowermost conductors. The result is a net field strength greater than zero in the pipe. In other words, even though the mathematical sum of the magnetic field is zero, the existing field in the pipe will be greater than zero. Mathematical expressions on how to determine this magnitude has not been analysed. It can, however, be concluded that eddy currents will rise in the pipe due to local field penetration in the pipe. Finally, if the induced current in the pipe were to be found, the heat loss could be expressed as:

$$P_{pipe} = \frac{1}{\sigma_{pipe}} \iint_A J^2 dA \tag{4.8}$$

In which:

P_{pipe}	is the loss in the pipe (W)
σ_{pipe}	is the electric conductivity in the pipe (S/m)
J	is the current density in the pipe (A/m^2)

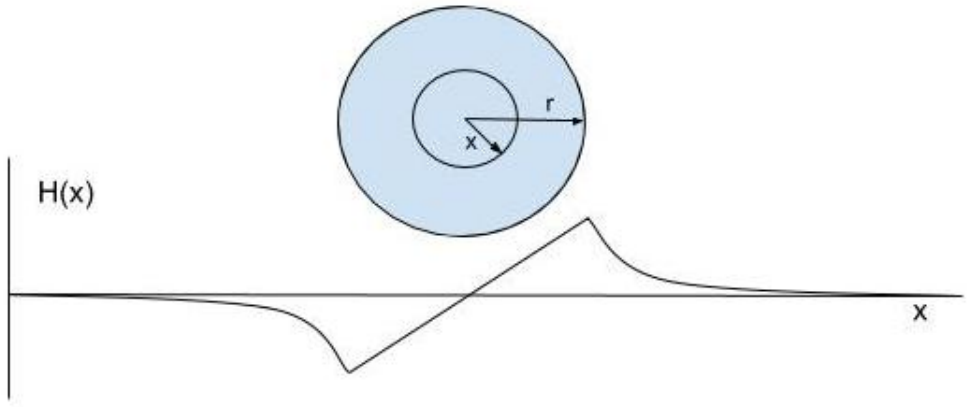

Figure 4.1: The magnetic field strength from a current carrying conductor as a function of distance

Chapter 5

COMSOL

COMSOL is based on nummerical methods. The software iterates over a set of equations in a numerical manner until the solution converge. This happens within the drawn geometry in the model, and the geometry is split up to something called a mesh. Within the mesh, thousands of nodes exists, and the equations are solved with respect to these nodes and to whatever exists between them. The mesh (and corresponding nodes) are called finite elements.
After a simulation has converged, each of these nodes contains a solution based on the applied equation. If desired, this solution can be collected from the node by simply asking the node for the answer. As an example, if the model contains 10.000 nodes, one will have access to just as many solutions. This could for example be the temperature in the conductor, pipe, sand or somewhere in between - all at once. On the contrary, by using the analytical approach (theory of mirrors), one will obtain *one* solution per calculation. This will obviously be very time demanding if several solutions are desired.

5.1 Boundary Conditions and Limitations

Once the geometry is drawn in COMSOL, on must apply the desired boundary conditions. These conditions are terms to the analysis, which COMSOL must know in order to obtain a solution. These terms vary according to the physics application, which must be chosen prior to a simulation. The physics used for this analysis is called *Heat Transfer in Solids* and *Magnetic Fields*. They contain all needed features for this analysis, such as a current source. The current source can also act as a heat source. The *Magnetic Fields*-branch was also used to simulate and obtain heat loss in the aluminum pipe. In addition, prior to running a simulation, COMSOL requests a study type (solver configuration). There are many varieties of studies to choose from, based on the desired solution. For this analysis, the selected studies were *Time Domain* and *Frequency Domain*. To fully run a simulation, COMSOL must know a minimum of boundary conditions prior to a simulation:

- Where in the geometry the heat transfer equation shall apply
- Where in the geometry Ampere‘s Law shall apply
- Initial values of temperature
- Heat sources
- The temperature to the ambient environment
- The desired heat mechanism to the ambient environment (isotherm or diffuse)
- Material parameters, such as thermal resistivity- and capacity, mass density, electrical properties etc.

For all simulations presented in this thesis, the heat transfer equation was applied to the entire model at all times, since heat flow appears everywhere in the model. The equation which COMSOL solves during a simulation is written as [14]:

$$\rho C_p \frac{\partial T}{\partial t} + \rho C_p \mathbf{u} \cdot \nabla T + \nabla \cdot \mathbf{q} = Q \tag{5.1}$$

In which:

ρ	is mass density (kg/m^3)
C_p	is the specific heat capacity at constant pressure (J/kg·K)
T	is temperature (K)
t	is time (s)
$\mathbf{u}$	is the velocity vector (m/s)
$\mathbf{q}$	is heat flux by conduction (W/m^2)
Q	is the heat source (or sink) (W/m^3)

Ampere‘s law was chosen to apply in the conductors and the aluminum pipe. The only exception was when applying the *frequency* study to obtain heat loss in the pipe, where Ampere‘s Law was applied to the entire geometry. When applying the *Time Dependent* solver, the exact equation which is solved in COMSOL becomes:

$$\sigma \frac{\partial \mathbf{A}}{\partial t} + \nabla x H = J_e \tag{5.2}$$

In which:

σ	is the electric conductivity (S/m)
$\mathbf{A}$	is the magnetic vector potential (Wb/m)
H	is the magnetic field strength (A/m)
J_e	is the externally applied current density (A/m^2)

And when applying the *Frequency Domain*, the equation becomes:

$$(j\omega\sigma - \omega^2\epsilon_0\epsilon_r)\mathbf{A} + \nabla xH = J_e \tag{5.3}$$

In which:

- ω = 2πf (rad/s)
- f is the frequency (Hz)
- ϵ_o is the permeability constant ($4\pi{\cdot}10^{-7}$ H/m)
- ϵ_r is the relative permeability

Both the conductors and the aluminum pipe was sat to represent the heat sources. As for the heat mechanism to the ambient environment, this was sat do be a diffuse surface. In practice, this means that the outer boundaries of the model was radiating heat to the ambient environment. This is absolutely more realistic compared to an isotherm surface, which would incorporate a constant temperature surrounding the models. This could be obtained by water cooling or by a somewhat similar technique. It was, however, chosen no to do this in the experiments, hence the simulations should reflect this by a applying a diffuse surface. In addition, all thermal properties in the COMSOL models were constant. This means that water vaporization (drying of the sand) was not taken into consideration.

In COMSOL, all simulations and geometries were exclusively treated in two dimensions (x and y direction in rectangular coordinates). This means that COMSOL sees the z-direction as infinitely long, hence no gradients of any kind occurs in the z-direction. In other words, all produced heat inside the COMSOL model must be transported via the x and y direction (radial), and no heat will ever be transported in the longitudinal direction. This is a clear limitation when compared to the experiments, where heat transport in the longitudinal direction obviously occurred due to temperature gradients.

5.2 Incorporated Parameters To COMSOL

As mentioned, COMSOL requires many parameters to be able to run a simulation. All parameters of relevance to the simulations are listed in table 5.1. The thermal conductivity, specific heat capacity and mass density of the soil were empirically obtained, and is being presented in 7. All other values were obtained from the default in COMSOL. XLPE did not exist as a default, but the thermal properties of XLPE are assumed to be equal to PVC.

Table 5.1: List over parameters incorporated to the simulations

Materials	Thermal conductivity (W/mK)	Specific heat capacity (J/mK)	Mass density (kg/m^3)	Electric resistivity (Ωm)	Relative permeability (1)
Soil	0.308/0.544	800	2106	-	-
Air	0.0259	1000	1.2	-	1
Wood	0.15	2300	1000	-	-
Conductors	238	900	2700	2.82 e-8	1
Aluminum pipe	238	900	2700	2.82 e-8	1
Plastic pipe	0.3	1900	930	-	-
XLPE	0.3	1900	930	-	-

Part II

Experiments and Data Collection

Chapter 6

Method

In order to obtain the desired data from the experiment, a reasonable, comparative and quantitative method must be chosen. To answer the problem description, there is a need to reach a relatively high conductor temperature, whereas the cables are placed in models which represents the cable plants of interest as described in the introduction. To achieve this, it was chosen to build 3 different models; one with cables placed directly in soil, and two with the cables placed inside a plastic- and aluminum pipe, respectively.

This chapter sums up and describes the choice for the method used in this experiment. Detailed descriptions about the models are presented in the upcoming sections, such as practical construction technique, a material list, installation of temperature monitoring equipment, power loss calculations and more.

6.1 A General Exposition For The Method

At the high current laboratory at NTNU, three single phased transformers are at disposal. They can be controlled to deliver a range of 0-10 kA at the secondary side, with an apparent power of 250 kVA per phase. Because of the accessibility to such good equipment, it was chosen to use this as a basis for the experiment, namely a current source for energizing the cables. Further, the idea was to terminate cables to the transformers in a loop, placing the cables inside the test objects (models), exclusively build for this purpose. The main benefit of connecting the models in series, is equal heat loss in the models. This is simply due to equal currents flowing through the cables, hence models, at all times during the experiment. To monitor and record the temperatures, the cables were equipped with thermal probes as being described in section 3.3. All probes were connected to a laptop computer for surveillance.

6.2 Choice Of Installation Design

To obtain the desired data, the design had to reflect the aluminum pipe-solution in comparison to other, more standardized laying techniques of power cables. Because of that, three different designs were designated for the experiment:

- Cables laid directly in sand, known as **model 1**
- Cables laid in a PVC pipe surrounded by sand, known as **model 2**
- Cables laid in an aluminum pipe surrounded by sand, known as **model 3**

The cable configuration of all the above mentioned designs, was chosen to be a trefoil formation. This was due to easier handing of the cables during the construction and installation. Many cables in the medium-voltage range are of the twisted single core type, such as the 22/11 kV TSLF cable. In other words, the trefoil formation is used by utilities today, and it was therefore an appropriate design for this experiment.

At real on-site cable plants, both cables and pipes are usually surrounded by cable sand in all directions from the cable[4]. The sand is often compressed by the help of heavy machinery. All of this is due to a more efficient cooling of the cable and for mechanical protection from rocks and other objects. For this experiment, however, it is chosen to not use cable sand, nor compress it. Mechanical protection was obviously not a concern in the experiment, and cable sand are in addition more expensive than ordinary sand. It was therefore chosen use standard, fine grained sand from a local builders merchant shop.

6.3 Experiment Representation

A representation of the complete experimental set up is shown in 6.3. One should note that the energy sources for the cables are represented as current sources. The reason for this is mainly the low impedance in the cables, which in practice is seen upon as a short circuit. A consequence of this, is a very low voltage, especially at moderate currents. It was therefore chosen to represent the energy sources as current sources.

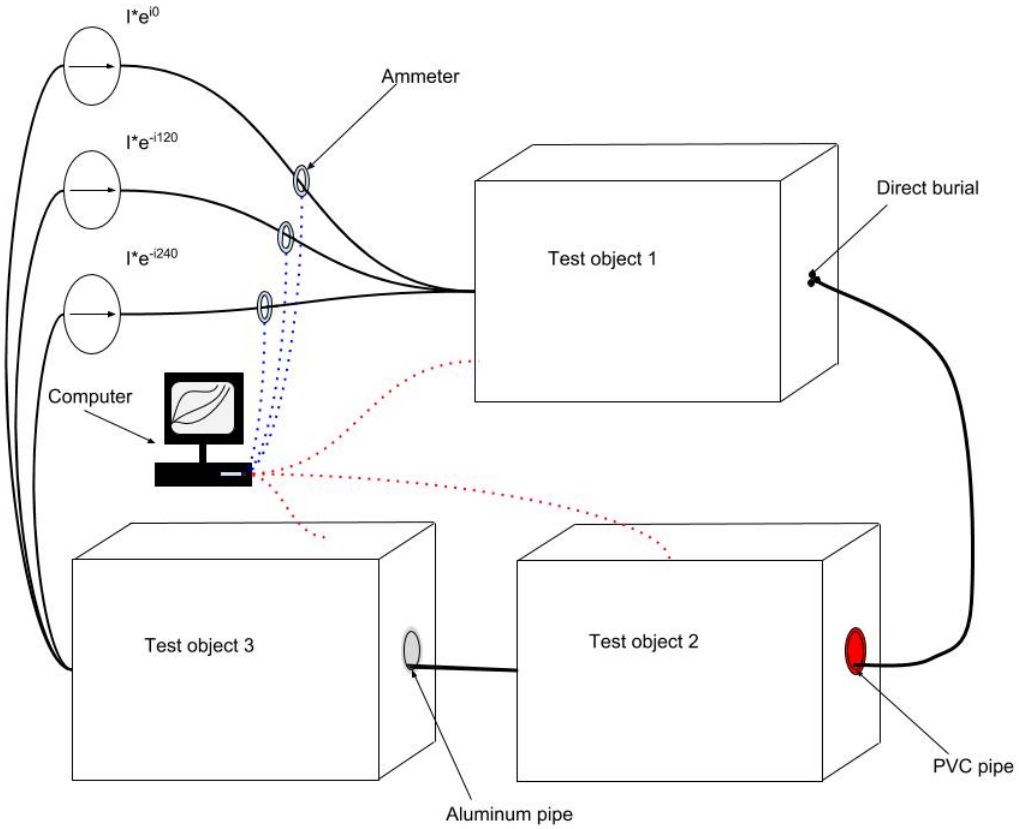

Figure 6.1: Animation of the experimental set up

6.4 Model Construction

The materials and equipment used for this experiment were based on the accessibility in the laboratory. As a base for the models, wooden pallets were found useful, measuring 75 x 115 cm. The walls of the models were assembled by wooden frame elements which was stacked to a height of 57 cm. To adapt the models to each design, holes were drilled in the middle of both short-ends of each box. Thereafter, the pipes were placed through the models, except for the one only containing sand. To avoid leakage of sand, tarpaulins were mounted inside all models, as it is being presented in Figure 6.4.

Figure 6.2: Tarpaulins were installed inside all models. The picture was taken before installing thermocouple probes.

Before the sand was applied to the models, several thermocouple probes were installed in the system. 19 probes were installed in direct contact with the uppermost conductor in the trefoil formation. This was obtained by the help of an electric drill. The diameter of the drill was 2 millimetres, and the depth of the holes in the insulation were just deep enough to reach the surface of the conductor. To secure the probes from slipping or being dislocated, a tiny drop of silicon was used in addition to a couple of turns with electrical tape. A representation of the location for each probe is being presented in Figure 6.4. The figure represents all models in the longitudinal direction, with model 1, 2 and 3 from left to right, respectively.

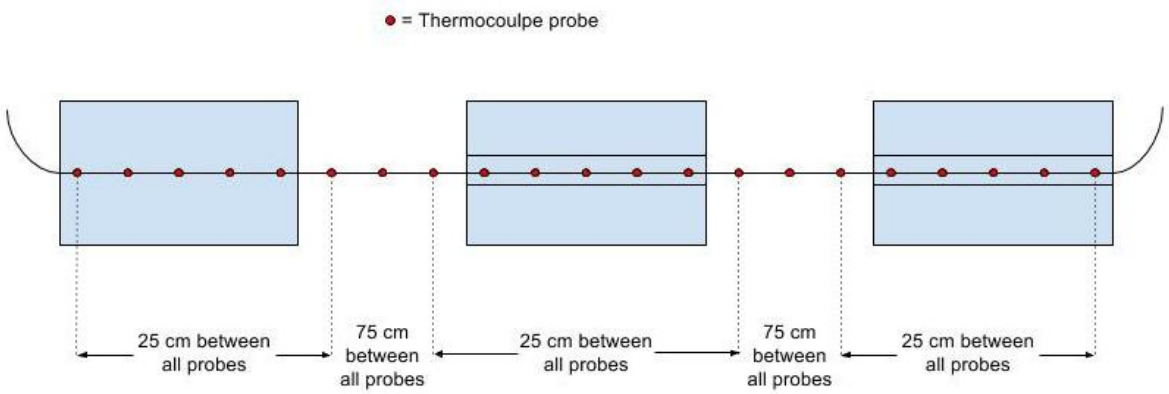

Figure 6.3: A representation of the location for each thermocouple probe inside the conductor.

Despite that the conductor temperature was highest emphasized in the experiment, probes were also installed in the radial direction in all models. The main reason for installing these probes was that other students can benefit of the models in future experiments, if wanted. These probes were installed in the middle of the models, lengthwise. 2 of these probes were placed horizontally away from the pipes, with 5 and 15 cm displacement from both pipes. The same displacement was installed in model 1. 2 probes were also installed in the vertical direction with the same displacement as the horizontal ones.
To monitor the temperature in the aluminum pipe, one probe was attached to the pipe at the top and bottom, in addition to both sides (four in total). This is being presented in Figure 6.4. In the PVC pipe, one probe was installed at the top, and one at the bottom of the pipe. Finally, one probe was attached at the top of the uppermost conductor, and one probe was placed in the center between the cables, as being presented in 6.5. The last mentioned was done in all three models. Figure 6.6 and 6.7 shows the same configurations in model 1. The probes are the blue dots.

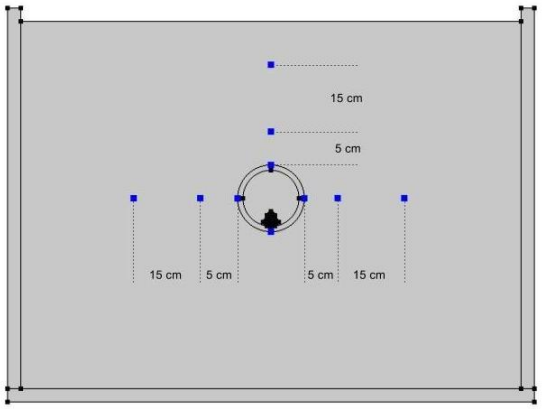

Figure 6.4: Location for external probes in x-y direction for aluminum- and plastic pipes.

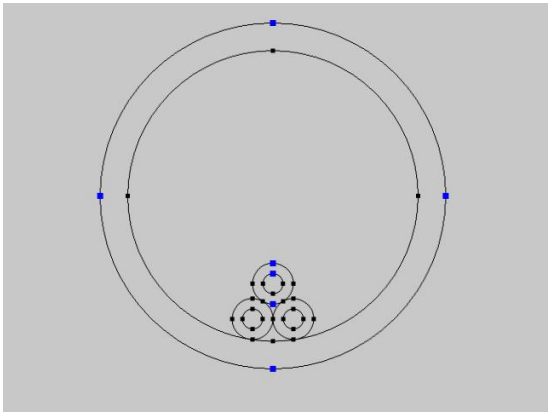

Figure 6.5: Placement of top- and center probe inside the aluminum- and plastic pipes.

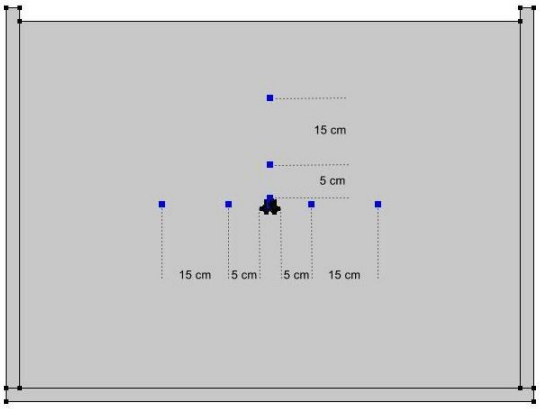

Figure 6.6: Location for external probes in x-y direction for direct laying in sand.

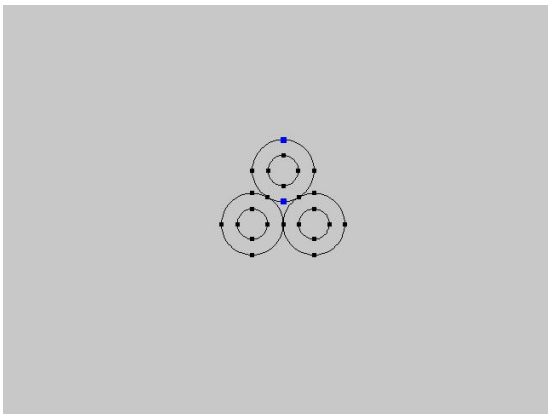

Figure 6.7: Placement of top- and center probe in direct laying in sand.

To align the above mentioned probes in the models, a system of tightly stretched fireline[1] was used. The probes were attached to the line with tape, and it is assumed that both the fireline nor the tape provided any interference regarding temperature measurements. An example of how the fireline was used, is shown in figure 6.8. As seen, the sand was carefully applied little by little to ensure that the probes stayed in place.

Figure 6.8: Assembling the probes by the help of fireline.

After the sand was applied to the models, a small amount of rockwool[2] was filled approximately 10 cm inside the pipes at both ends of the pipes. In addition, plates of styrofoam was

[1]Fireline is a multifilament fishing line with a superbly high rupture strength.
[2]Rockwool (or glava) is a type of insulation used for all types of buildings.

installed at both ends, covering the whole area of the boxes as being presented in Figure 6.4. The intention behind this action was to limit heat fluctuations in the z-direction, meaning in the longitudinal direction. If this was to succeed, most heat loss from the cables should be forced in the radial direction. This is the way the 2D-simulations in COMSOL are calculated, where all heat flow propagates in the x- and y directions as described in section 5.1. Finally, a transparent plastic sheath was wrapped on top of the models to avoid leakage of water vaporization. This was an attempt to keep the thermal conductivity constant during the experiment, since drying of sand leads to decreased thermal conductivity.

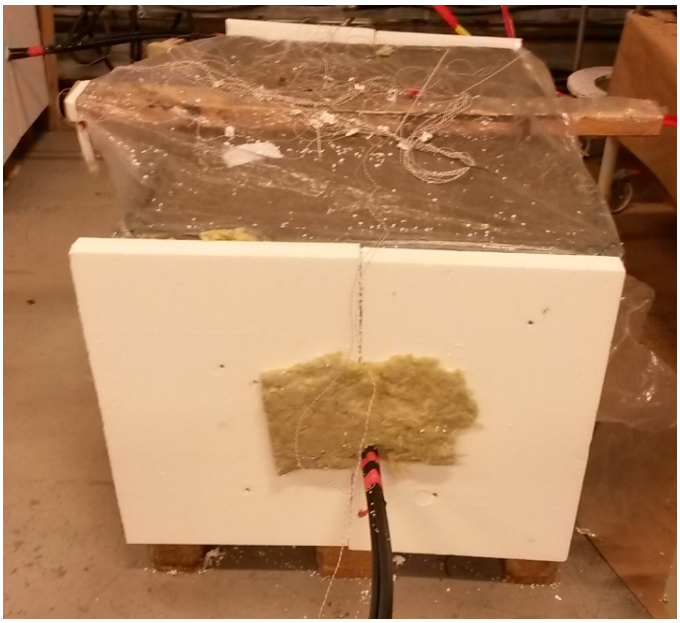

Figure 6.9: One of the models after installing styrofoam and rockwool.

6.4.1 Material List

The complete list of materials and equipment used for this experiment are listed as follows:

- Three single phase transformers, ESTTK-O (National Transformer), 250 kVA.
- Three single phase voltage stabilizers, VDE 0552 (Ruhstrat), 250 kVA.
- Three single phased XLPE 7.2 kV 25 mm^2 Al cables.
- Three wooden pallets, 75x115 cm.
- Nine stackable wooden frames for the pallets (19 cm high).
- Approximately 2 m^3 of sand.
- One aluminum pipe with a diameter of 100 mm and wall thickness of 8 mm.
- One PVC pipe with a diameter of 110 mm and wall thickness of 6 mm.
- Plastic tarpaulins.
- One Agilent 34972A LXI Switch Unit.
- A laptop with recording software compatible with the switch unit.

- Temp T - thermocouple probe wire.
- Hukseflux Thermal Sensors (for measuring thermal conductivity).
- Fluke Visual IR Thermometer.
- Fluke 336 Ammeter.
- Fluke 1000s AC Current Probe.
- Miscellaneous construction materials and tools (nails, duct tape etc).

6.5 Heat Loss Measurements

It is obviously very important to measure the generated heat loss at all times during the experiment. This can easily be done by measuring the current. It can also be done by measuring the voltage, but the current technique has the greatest benefits for this experiment.
First, if a voltage was to be measured, it could only be measured over the secondary sides of the transformers, and not over the test objects (models). Secondly, there would be a need of an oscilloscope in the system to measure ϕ, the phase angle between voltage and current, due to the inductive parameters of the circuit. Thirdly, the need for an oscilloscope would increase the complexity of the experiment. Finally, if this technique was used, one would only know the total generated loss in the cables, and not the loss inside the the test objects. On the other hand, one could calculate the heat dissipation in the models using the *voltage divider rule*, but current measurements seems more accurate for this purpose. By only measuring the current, one can easily obtain the generated heat loss per unit length. For three conductors, the equation becomes:

$$P = 3I^2R_{AC} \tag{6.1}$$

The heat loss within the constraints of the models can afterwards be obtained by multiplying the heat loss per unit length, by the length of the model. Because of its flexibility and accuracy, the I^2R technique was chosen for this experiment. The current was measured using one ammeter per phase (see the material list).

6.5.1 Measurement of Losses in the Aluminum Pipe

As indicated in section 4.1, there will be induced eddy currents circulating in the pipe, and they will generate a heat loss. However, these currents can not be measured by applying a clamp-meter (ammeter) around the pipe. The reason for this, is that the vectorial sum of the currents are equal to zero, since the magnetic fields equals to zero. Nevertheless, the produced heat in the pipe can be calculated by the following equation [5]:

$$P = mc\frac{\partial \Theta_p}{\partial t} \tag{6.2}$$

Where:

P	is power loss (W)
m	is the mass of the object (kg)
c	is the specific thermal capacity of the material (J/kg·K)
$\frac{\partial \Theta_p}{\partial t}$	is the rate of change in temperature with respect to time in the pipe (K/s)

The mass of the aluminum pipe is easily calculated as:

$$m_p = \rho_p V_p = \rho_p \pi (r_{outer}^2 - r_{inner}^2) l \tag{6.3}$$

This particular technique was used in [13] to measure heat loss in metallic pipes. It is important to measure $\partial \Theta_p$ in the pipe during a short transient, preferably at the start of the experiment, under the assumption that the heating is adiabatic. If external heat transfer to or from the pipe was a part of $\partial \Theta_p$, it would be hard to determine the magnitude caused by eddy currents, and the magnitude caused by external heat transfer. In [13], a time of 40 seconds was used to determine this temperature rise. They also incorporated the average temperature rise in the pipe, since the temperature differed in a circumferential distribution in the pipe.

Chapter 7

Preliminary Measurements

7.1 Measured Heat Loss in The Aluminum Pipe

The generated heat loss was measured at the very beginning of the experiment according to 6.5.1. The temperatures were obtained by the four thermocouple probes attached to the pipe as described in section 6.4. To ensure that the temperature rise in the pipe was properly obtained, the temperatures were measured for 300 seconds. This was determined due to some thermal inertia in the pipe, but hopefully within the reach of an adiabatic process. The measured temperatures with respect to time and the given probes are shown in figure 7.1.

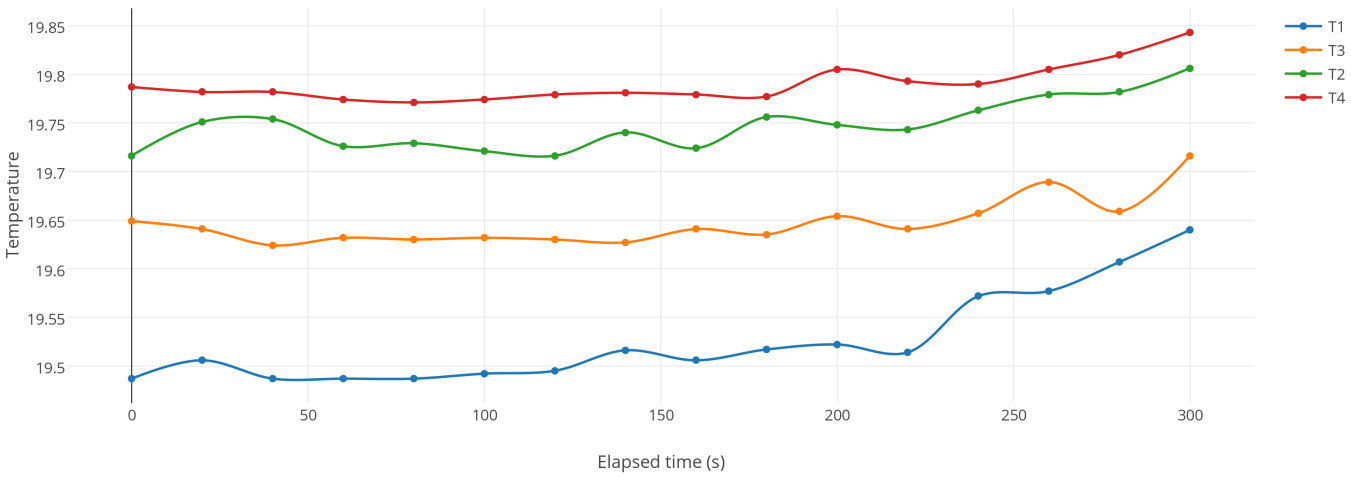

Figure 7.1: Temperature rise in the aluminum pipe after the current was applied.

The average temperature rise in the pipe can be calculated as:

$$\Delta\overline{\Theta}_{pipe} = \frac{\sum_{n=1}^{n} \Delta\Theta_i}{n} \tag{7.1}$$

And the various temperature differences between $0s < t < 300s$ were:

- $\Delta\Theta_1 = 19.64 - 19.48 = 0.16\,^{\circ}\mathrm{C}$
- $\Delta\Theta_2 = 19.80 - 19.71 = 0.09\,^{\circ}\mathrm{C}$
- $\Delta\Theta_3 = 19.35 - 19.29 = 0.06\,^{\circ}\mathrm{C}$
- $\Delta\Theta_4 = 19.84 - 19.78 = 0.06\,^{\circ}\mathrm{C}$

This gives an average temperature rise of:

$$\Delta\overline{\Theta}_{pipe} = \frac{\sum_{n=1}^{n} \Delta\Theta_i}{n} = \frac{0.16 + 0.09 + 0.06 + 0.06}{4} = 0.0925\,^{\circ}\mathrm{C} \tag{7.2}$$

To calculate the heat loss in the pipe, one also needs the mass of the pipe. The mass density of aluminum is approximately $2700(kg/m^3)$ [5]. Inner- and outer radius of the pipe was 44 and 50 mm respectively, and the length of the pipe was 1.3 meters. With this in mind, the mass becomes:

$$m_p = \rho_p V_p = \rho_p \pi (r_{outer}^2 - r_{inner}^2) l = 2700\pi(0.05^2 - 0.044^2)1.3 = 6.22(kg) \tag{7.3}$$

The isobaric heat capacity of aluminum is approximately $900(J/kgK)$ [5], so the heat loss in the pipe becomes:

$$P_{pipe} = m_p \cdot c_{alu} \cdot \frac{\Delta\overline{\Theta}_{pipe}}{\Delta t} = 6.22 \cdot 900 \cdot \frac{0.0925}{300} = 1.72(W) \tag{7.4}$$

If this stands correct, the induced heat loss in the pipe per unit length becomes:

$$P_{pipe/m} = \frac{P}{length} = \frac{1.73}{1.3} = 1.33(W/m) \tag{7.5}$$

7.2 Specific Heat Measurements

The specific heat capacity was obtained in coherence with the theory presented in section 3.4. The equipment which was used for this experiment is shown in figure 7.2. In addition, a water boiler was used to obtain different temperatures of the water. The box to the right in the picture is a sample of the soil, and the other objects are a scale, a thermometer and a thermal mug.

Figure 7.2: Equipment used for measuring the specific heat capacity in the sand.

Two different attempts were conducted with more or less arbitrary masses and temperatures of the soil and the water. This was to ensure correct results, as well as verifying the theory presented in 3.4. For both attempts, water was heated up and added to the room tempered soil. The pre- and post temperature values were measured, and the obtained results are shown in table 7.1. The final result is rounded down to 800 (J/kg·K), which was used in the simulations.

Table 7.1: Results from heat capacity measurements

	Attempt 1		**Attempt 2**	
Sand (Pre mass- and temperature)	200 g	22.2°C	402 g	21.6°C
Water (Pre mass- and temperature)	216 g	76.7°C	366 g	70.0°C
Resulting temperature when blended	68.5°C		62.1°C	
Specific heat capacity of water	4190 (J/kg·K)		4190 (J/kg·K)	
Calculated heat capacity of the sand[1]	**801.43 (J/kg·K)**		**800.63 (J/kg·K)**	

[1]Based on equation 3.22.

7.3 Thermal Conductivity Measurements

Values of thermal conductivity (W/m·K) was needed for simulations in COMSOL. It was therefore chosen to measure the thermal conductivity in the sand, both prior to, and after the water was added. The measurements were performed by the use of a *Hukeflux Thermal Sensors* machine. A Hukseflux-machine obtains the data from a probe, which measures temperature gradients while it produces heat. It was attempted to measure the conductivity in all models. Six measurements were performed (two in each model). Unfortunately, some of the measurements were unsuccessful due to technical errors.

Prior to adding water, the measured values of thermal conductivity was between 0.137 and 0.308. Some of these measurements gave no results at all (errors). After adding the water, the first four measurements had an average of 0.544, and the last two were 0.205 and 0.207, respectively.

The first four values after adding the water, were reasonable values considering that they were quite even, and also much higher than the obtained values from before adding the water. The last two values, however, was directly illogical, considering that equal amounts of water was added to all models. This is considered as a measurement-error in the probe. For example, if the probe had a disadvantageous angle when placed in the soil, a minor air gap could have occurred between the sand and the probe. This would lead to an equivalent lower conductivity, as seen from the probe. The highest values are therefore assumed to be the most correct values. It is therefore chosen to use the highest obtained values for the simulations, which was 0.308 (W/m·K) and 0.544 (W/m·K), respectively.

Chapter 8

Experiment Execution

8.1 Experiment Part 1 - Initial Attempt

A current of approximately 82 A was applied at the same instant. This current was running continuously for 100 hours before turning it off, but the conductor temperature stabilized at around 60 hours. The voltage stabilizers which controlled the currents, turned out to be quite sensitive to adjust. Because of that, it became almost impossible to obtain 100% balanced currents, but the deviations were very low. Prior to the experiment, all temperatures were at equilibrium, meaning room tempered at $\approx 20\,^{\circ}\mathrm{C}$.

8.1.1 Results From Part 1

The conductor temperatures as well as the applied currents are being presented in figure 8.1. The 3 conductor temperatures were obtained from the center of all models, and from the uppermost conductor in the trefoil formation.
To assess the trustworthiness and goodness of the entire experiment, the temperature in the longitudinal direction is of great importance since it provides information regarding transport of heat. Figure 8.2, presents the temperature in the longitudinal direction of the cable, obtained by a total of 19 thermocouple probes. The 6 different graphs presents these temperatures at different elapsed times into the experiment (0 to 95 hours). In figure 8.2, the different models are located at:

- 0 to 1 meter: model 1
- 2.95 to 3.95 meters: model 2
- 5.75 to 6.75 meters: model 3

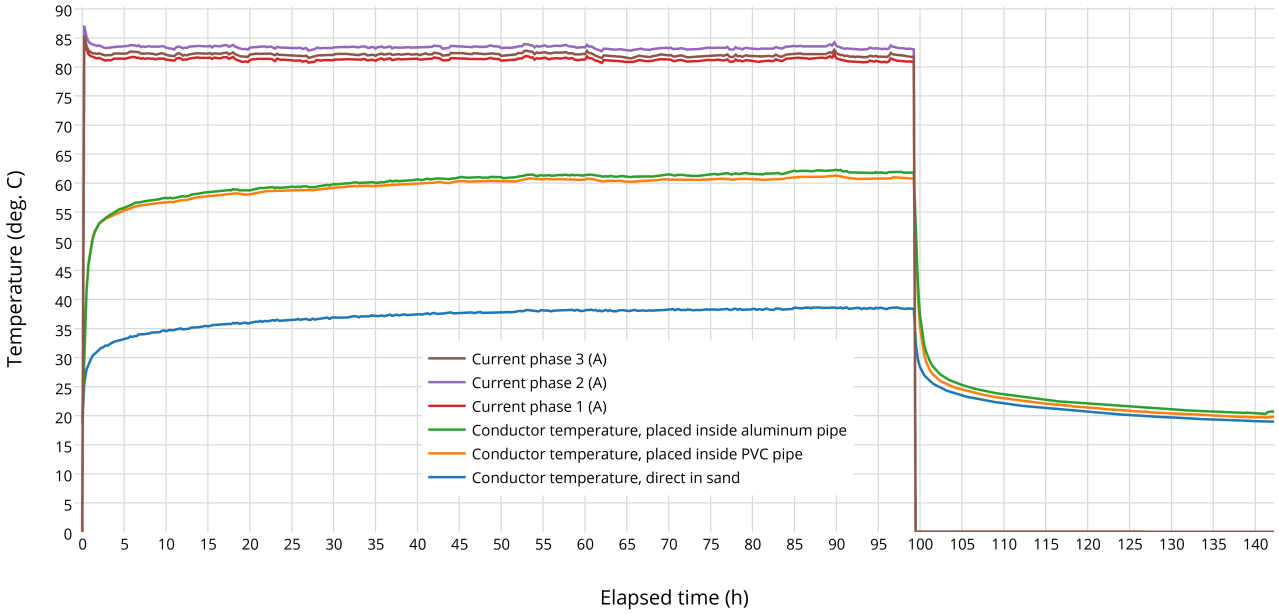

Figure 8.1: Conductor temperatures during the first 140 hours.

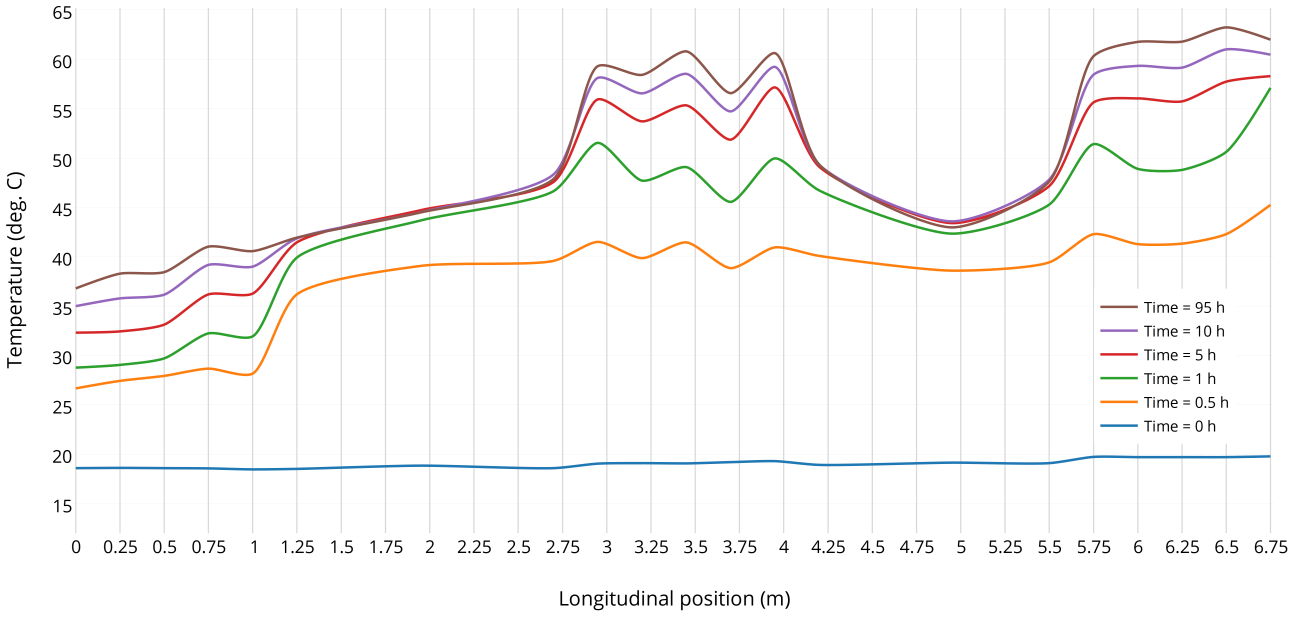

Figure 8.2: Longitudinal conductor temperature from experiment 1.

8.2 Experiment Part 2 - Increased Contact Surface

After reviewing the first experiment, it became necessary to take action regarding the low difference in conductor temperature between model 2 and 3. Surprisingly, both figure 8.1 and 8.2 proved that the temperature inside the aluminum pipe became slightly higher compared to the plastic pipe. During an investigation of the models, it became clear that the cables inside both pipes were not in direct contact with the bottom of the pipes at all locations, but rather with small gaps and unevenness. This was due to the stiffness and light weight of the cables, as they proved to hard to mount in the right place, meaning at the very bottom of the pipes.

It became of interest to investigate the impact of forcing the cables to the very bottom of both pipes, with good physical contact. It was chosen to do this by applying wooden planks in the pipes which fitted perfectly, thus forcing the cables to the bottom of the pipes. The wood was installed as shown in figure 8.3 and 8.4.

Figure 8.3: Plastic pipe

Figure 8.4: Aluminum pipe

Afterwards, a current of approximately 82 A was applied, just as in 8.1. The current was applied for 22.5 hours before turning it off.

8.2.1 Results From Part 2

Figure 8.5 presents the measured conductor temperature at the center of each model. Figure 8.6 presents the longitudinal conductor temperatures at 5 different points in time. The location of the models are the same as in 8.1.

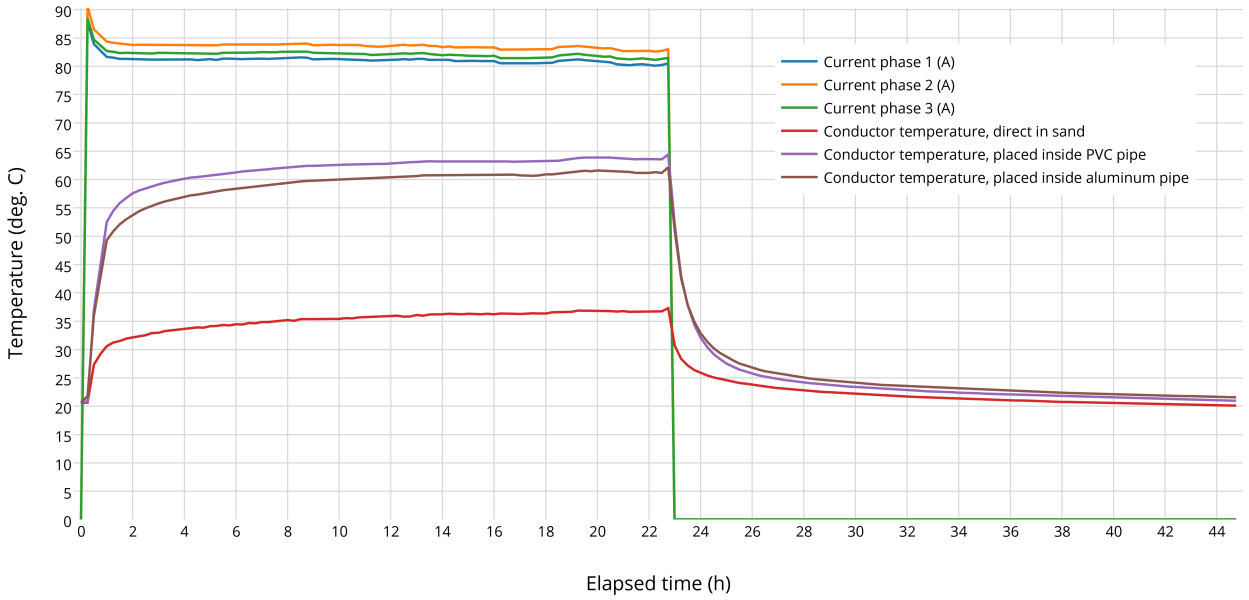

Figure 8.5: Measured conductor temperatures from experiment part 2.

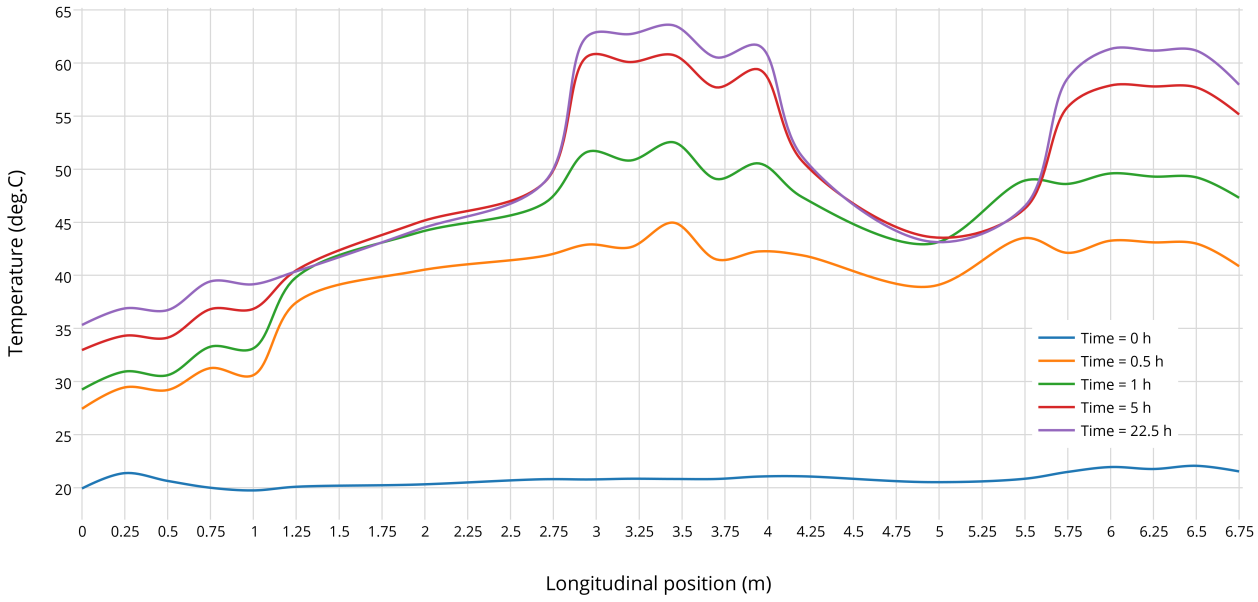

Figure 8.6: Longitudinal conductor temperatures from experiment part 2.

8.3 Experiment Part 3 - Adding Water To The Sand

Even with forced contact between the cables and the pipes, the results from part 2 still deviates quite much from the findings in [8], which indicated a difference in temperature up to 24 % between the plastic- and aluminum pipe. The attention was fully paid to revealing the reason for the large deviation. It became suspected that the low thermal conductivity in the sand could be one reason, simply because it dominated the total thermal conductivity in the system. At this point in time, the sand was completely dried out, and it is known that dry sand has a lower thermal conductivity than moist sand. It was therefore chosen to add water to the models to provoke a higher thermal conductivity. Equal amounts of water was added to the sand in the models, approximately 30 litres in each. To avoid or limit evacuation of water vapour from the models, all of the models were covered with thin plastic sheets at the top. This was an attempt to keep the thermal conductivity in the models constant with time during the conduction of the experiment. Before energizing the cables, the temperature in all models were at equilibrium, meaning room tempered at $\approx 20\,^{\circ}\mathrm{C}$. As a criterion to this part of the experiment, it was chosen to apply several step changes of load to the cables.

8.3.1 Results From Part 3

Different currents were applied for a total of 148 hours, and the resultant temperatures in the middle of each model are presented in table 8.1. These temperatures were obtained at the very last moment before changing the currents, since they were considered as the most stationary temperatures during the given time period. Please note that the obtained currents in table 8.1 are approximate, since they were found very difficult to control.
All details regarding the conductor temperatures are being presented in series in figures 8.7, 8.8, 8.9 and 8.10. That is, figure 8.8 is the continuation of figure 8.7, and so on.

In addition, the conductor temperature in the longitudinal direction is being presented in Figure 8.11. The two graphs were obtained during the highest and lowest applied currents, representing the extremal conditions of the experiment.

Table 8.1: Applied currents at different times during experiment part 3.

		Final value of conductor temperature (°C)		
Time period (hours)	Current (A)	Direct in sand	In PVC pipe	In aluminum pipe
$0 \rightarrow 49$	82	37.65	65.14	61.48
$49 \rightarrow 52.5$	97	42.57	82.24	77.45
$52.5 \rightarrow 94.5$	65	32.69	51.14	48.61
$94.5 \rightarrow 100.5$	115	50.55	107.48	99.75
$100.5 \rightarrow 148$	0	20.77	20.98	21.64

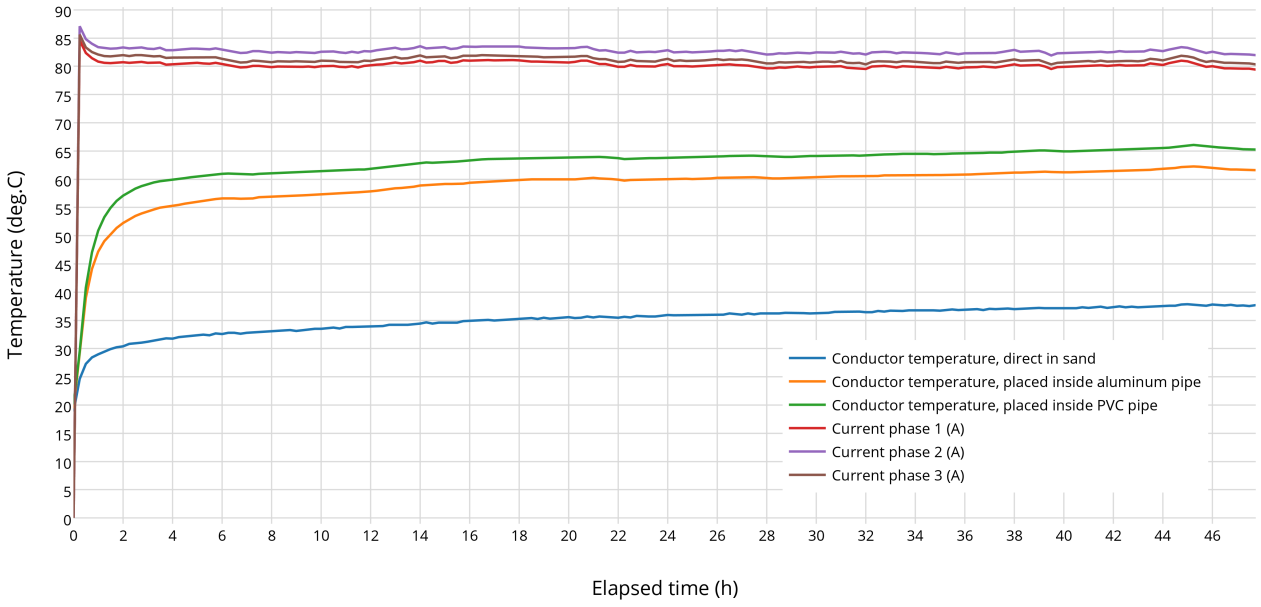

Figure 8.7: Conductor temperatures during experiment part 3 (0 to 48 hours).

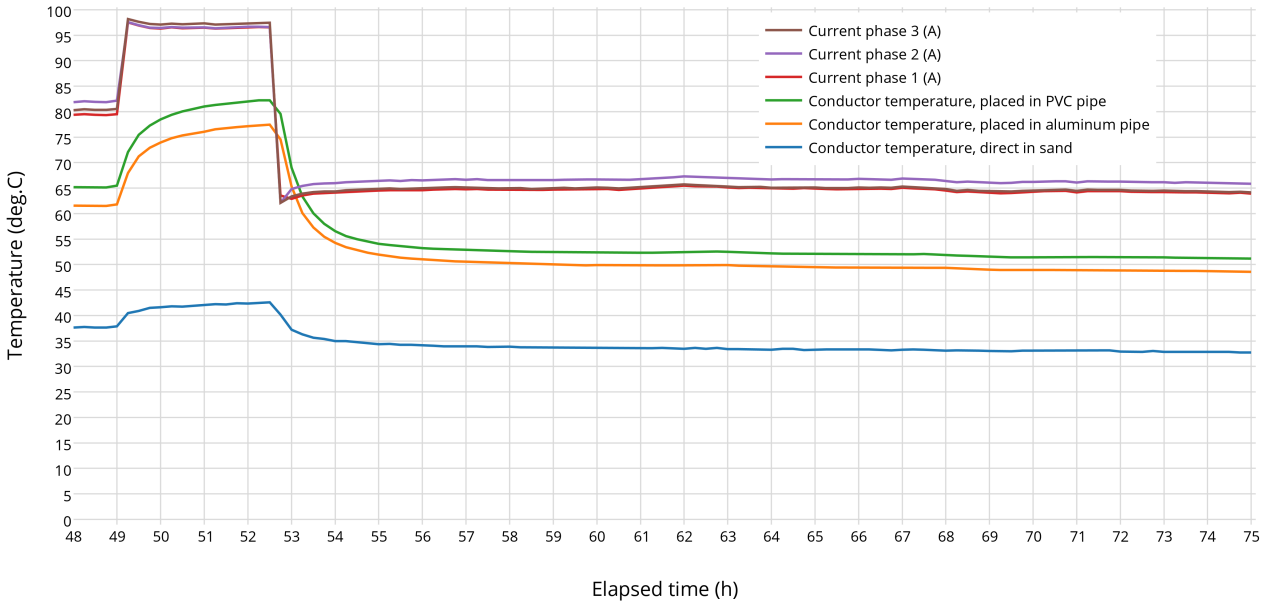

Figure 8.8: Conductor temperatures during experiment part 3 (48 to 75 hours).

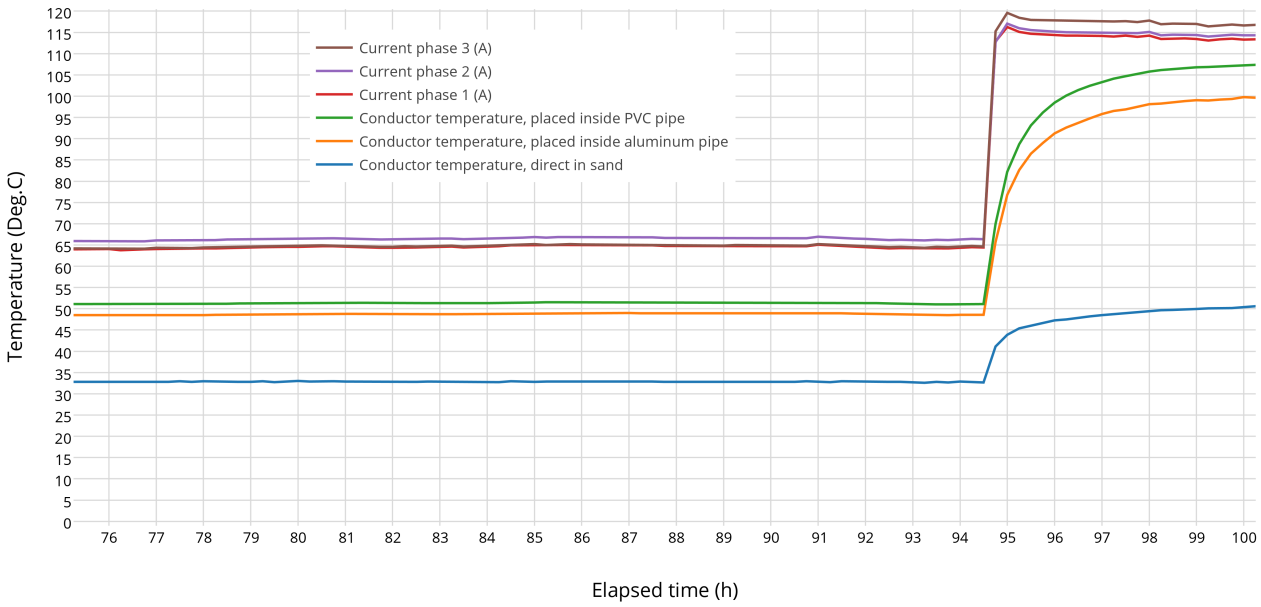

Figure 8.9: Conductor temperatures during experiment part 3 (75 to 100 hours).

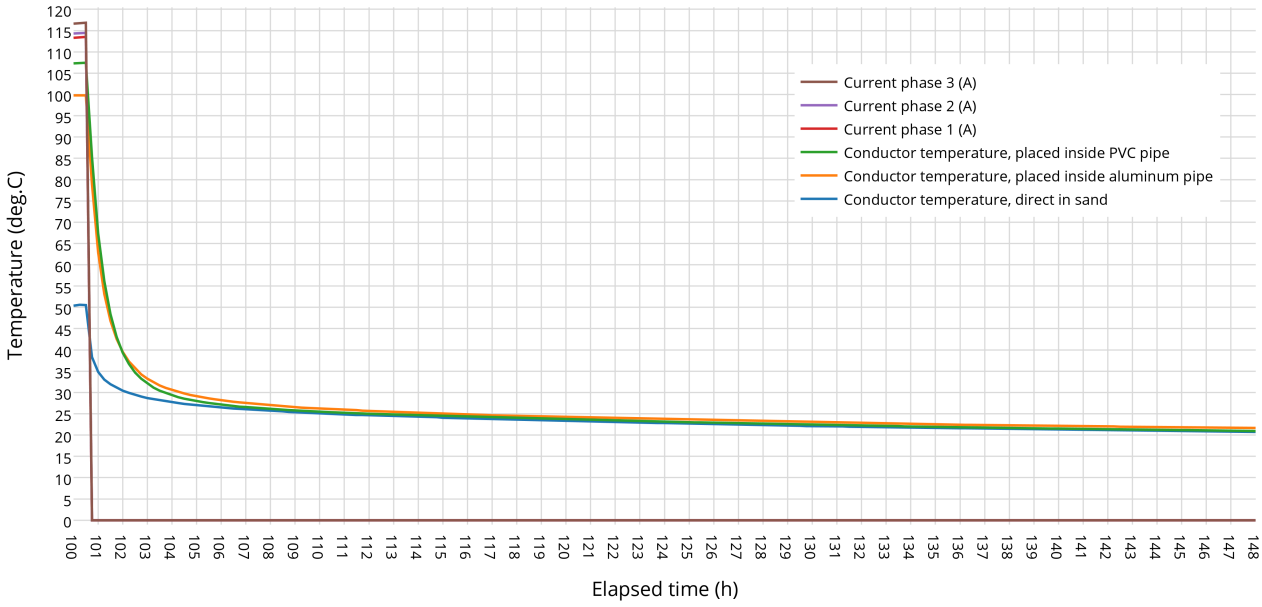

Figure 8.10: Conductor temperatures during experiment part 3 (100 to 148 hours).

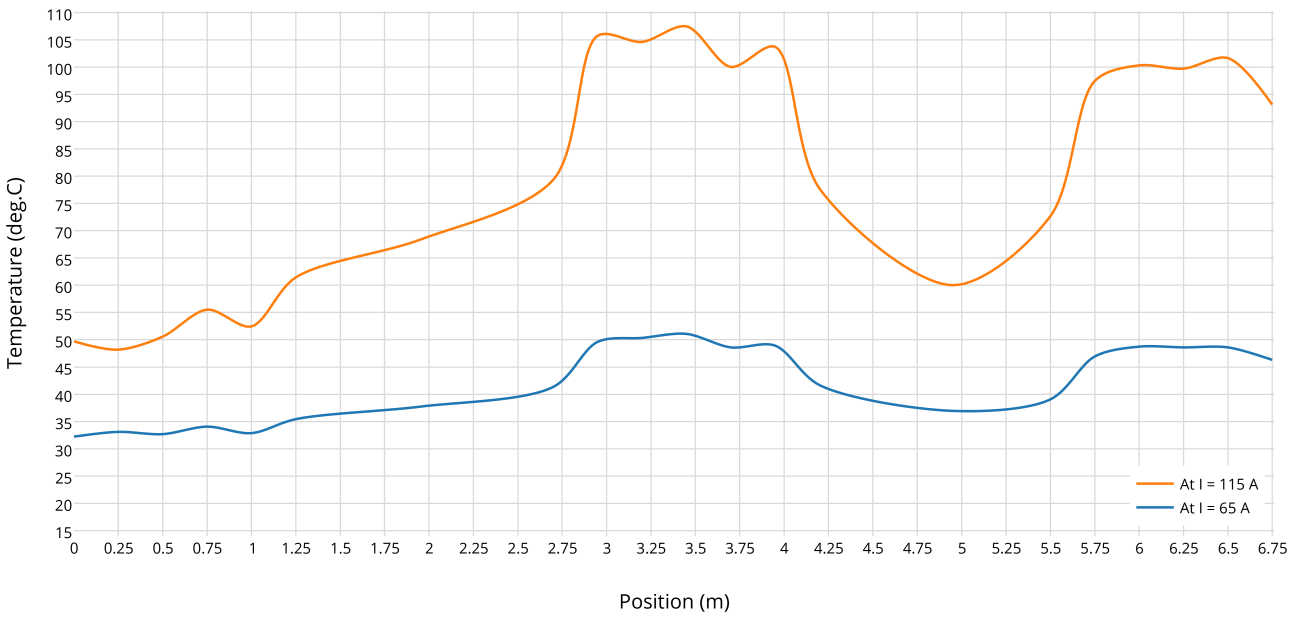

Figure 8.11: Longitudinal conductor temperatures during experiment part 3.

In figure 8.11, the different models are located at:

- 0 to 1 meter: cables placed directly in sand
- 2.95 to 3.95 meters: cables placed inside the plastic pipe
- 5.75 to 6.75 meters: cables placed inside the aluminum pipe

Chapter 9

Simulations

This chapter contains results from computer simulations as a second opinion to the experiments. The objective of simulating the experiments, is to reveal possible deviations between analytical computations and the results from the experiments.

It was not necessary to simulate all scenarios from the experiments to reveal deviations. It was therefore chosen to present *one* simulation of each model prior to, and after the water was applied (six in total). It is assumed that the thermal resistance in the soil was equal in experiment part 1 and 2, and it was therefore chosen to only simulate experiment part 2 as a reference to dry sand, and experiment part 3 as a reference to wet sand. In experiment part 2 and 3, a current of approximately 82 A was applied for 22.5- and 49 hours, respectively. To ease the analysis, it was chosen to simulate both part 2 and 3 for 22.5 hours, and to draw out data from the same period of time from the experiments. These two graphs are presented in the same diagram for each model and scenario (wet and dry).
The applied current is left out from the graphs, but in all graphs, the applied current in all phases are 82 A. The three different models were drawn as equal as possible to the real-life models. The remainder of boundary conditions were sat according to subsection 5.1. In addition to simulating the experiments, the heat loss in the aluminum pipe was also simulated.

9.1 Simulation Of Heat Loss In The Aluminum Pipe

To obtain the heat loss in the aluminum pipe, a *frequency domain* was applied to the COMSOL solver. By doing this, one can permit alternating currents in the simulations which is a condition to obtain induced currents, according to Faradays‘s Law. To simulate the exact same condition as in 7.1, a current 82 A was applied at 50 Hz. The loss in the pipe was simulated to 0.0856 (W/m) whereas the conductor losses were 7.177 (W/m) per phase, as being presented in Figure 9.1. Due to the negligible loss in the pipe, in became

of interest to investigate how dependant the heat loss in the pipe were as a function of the applied load current. The pipe loss was therefore simulated as a function of current in the range of $0 \leq I_c \leq 400$ A. The result is shown in Figure 9.2.

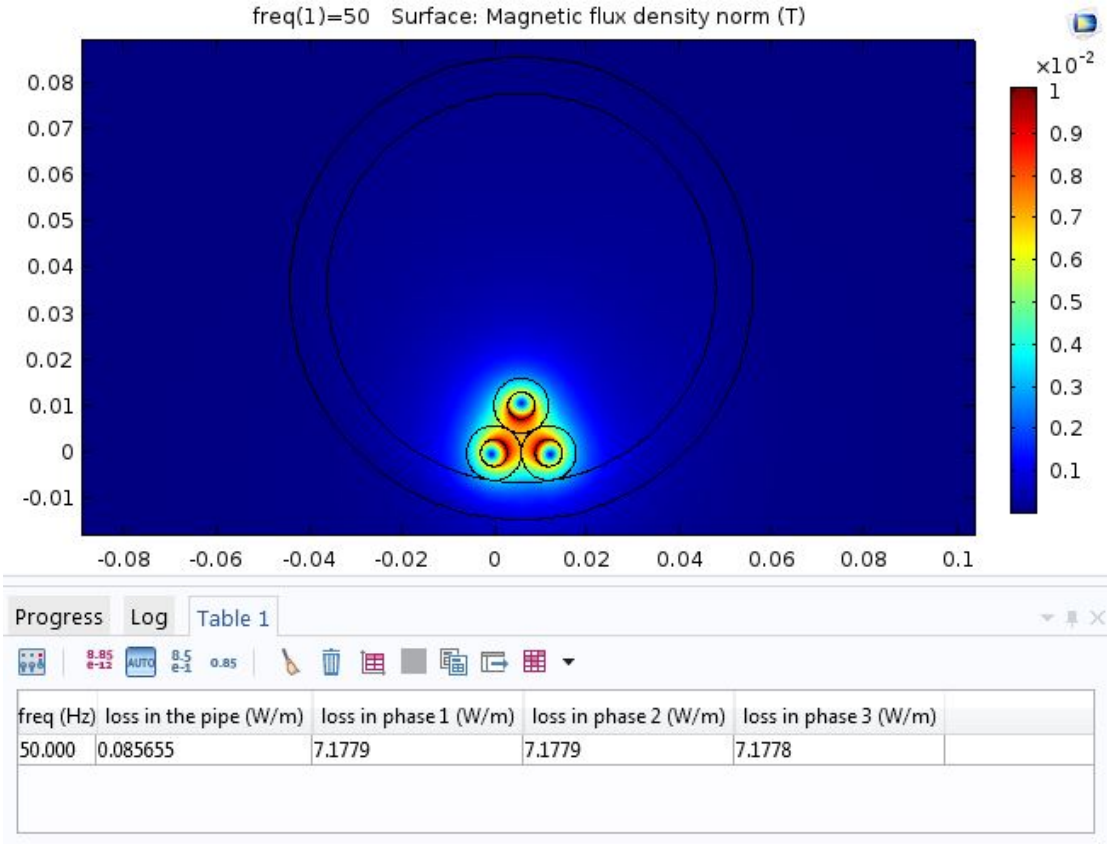

freq (Hz)	loss in the pipe (W/m)	loss in phase 1 (W/m)	loss in phase 2 (W/m)	loss in phase 3 (W/m)
50.000	0.085655	7.1779	7.1779	7.1778

Figure 9.1: A presentation of heat loss simulations in COMSOL. The results are listed in the table under the model.

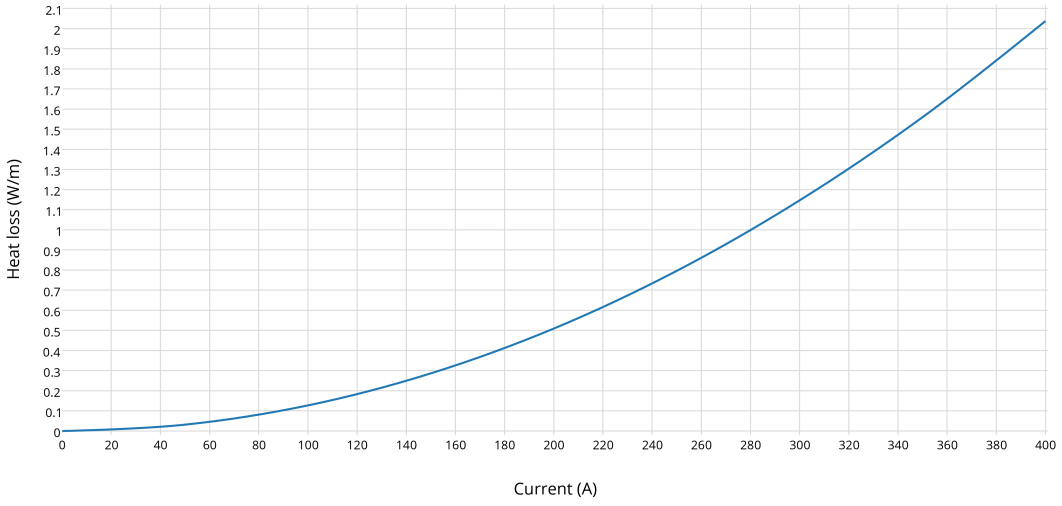

Figure 9.2: Simulated heat loss in the aluminum pipe as a function of conductor current at 50 Hz.

9.2 Direct Burial in Sand - Simulation Compared to Experiment

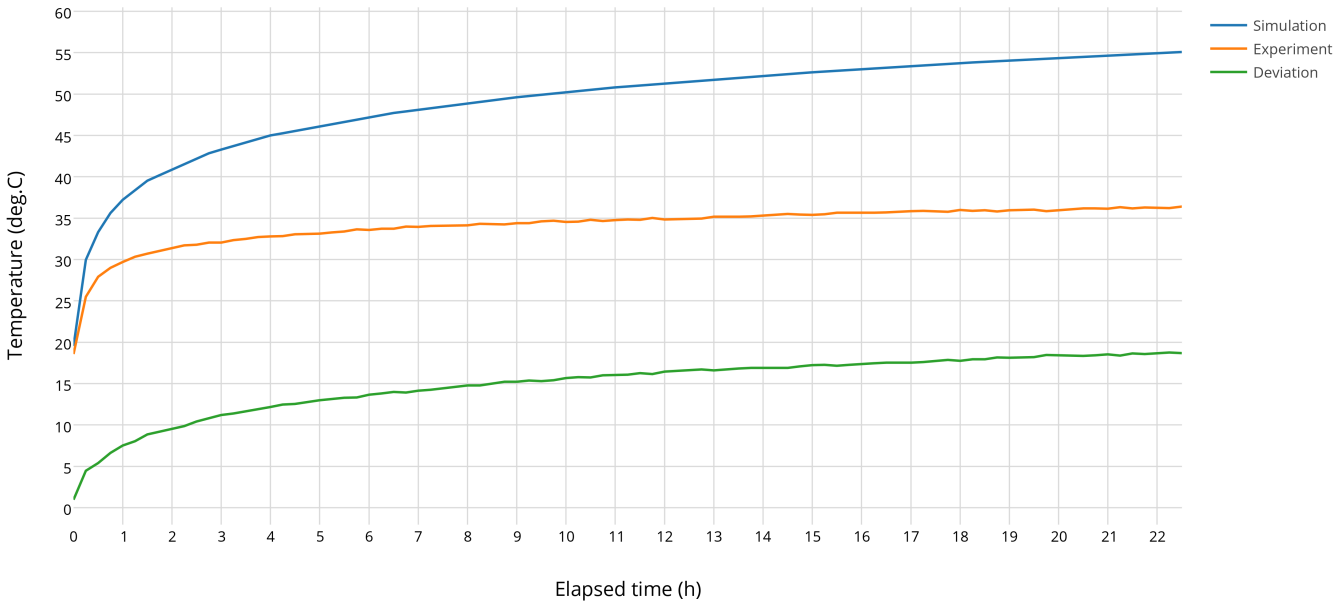

Figure 9.3: Before adding the water, model 1.

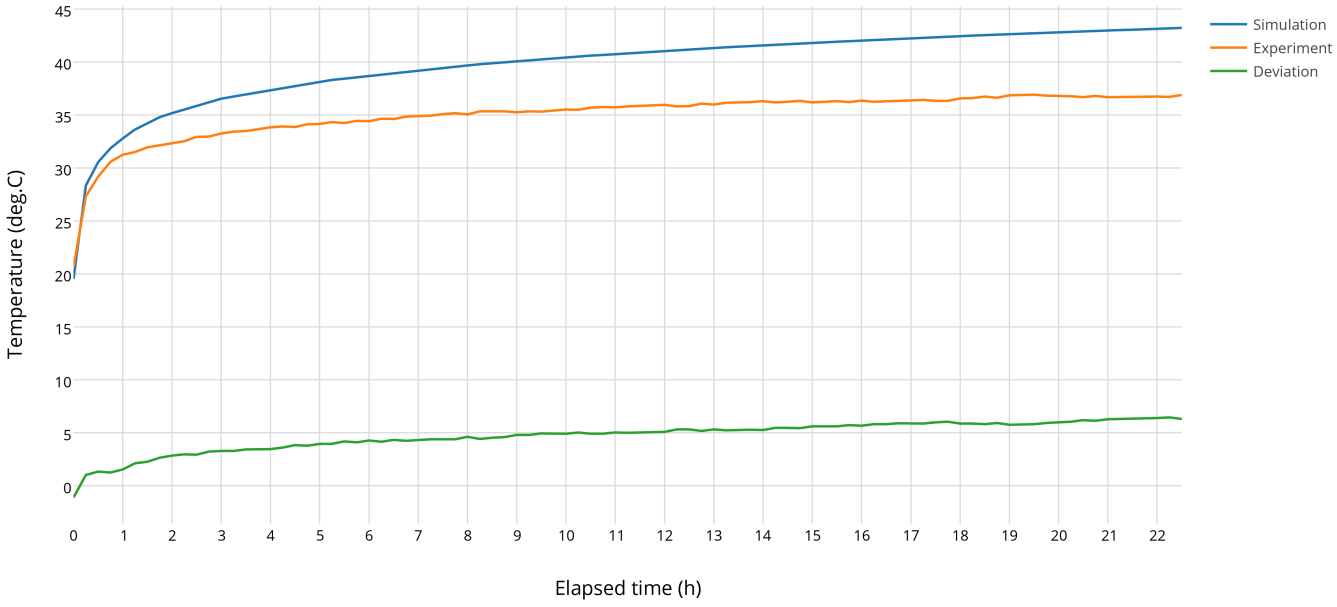

Figure 9.4: After adding the water, model 1.

9.3 Installation in PVC pipe - Simulation Compared to Experiment

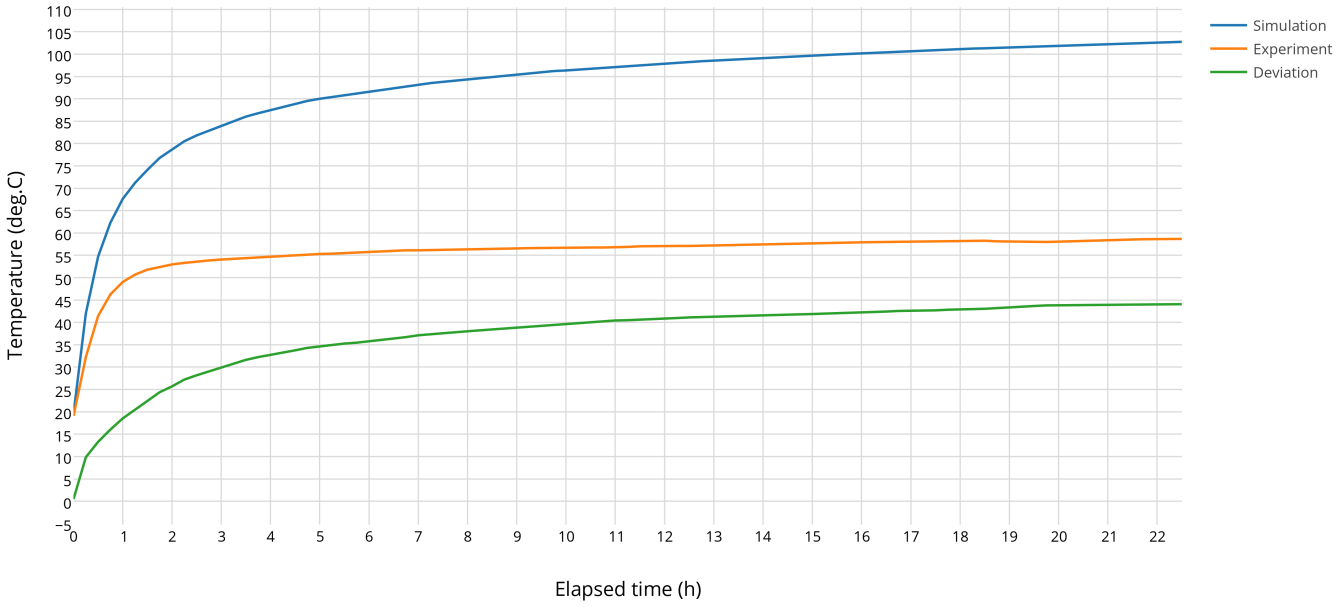

Figure 9.5: Before adding the water, model 2.

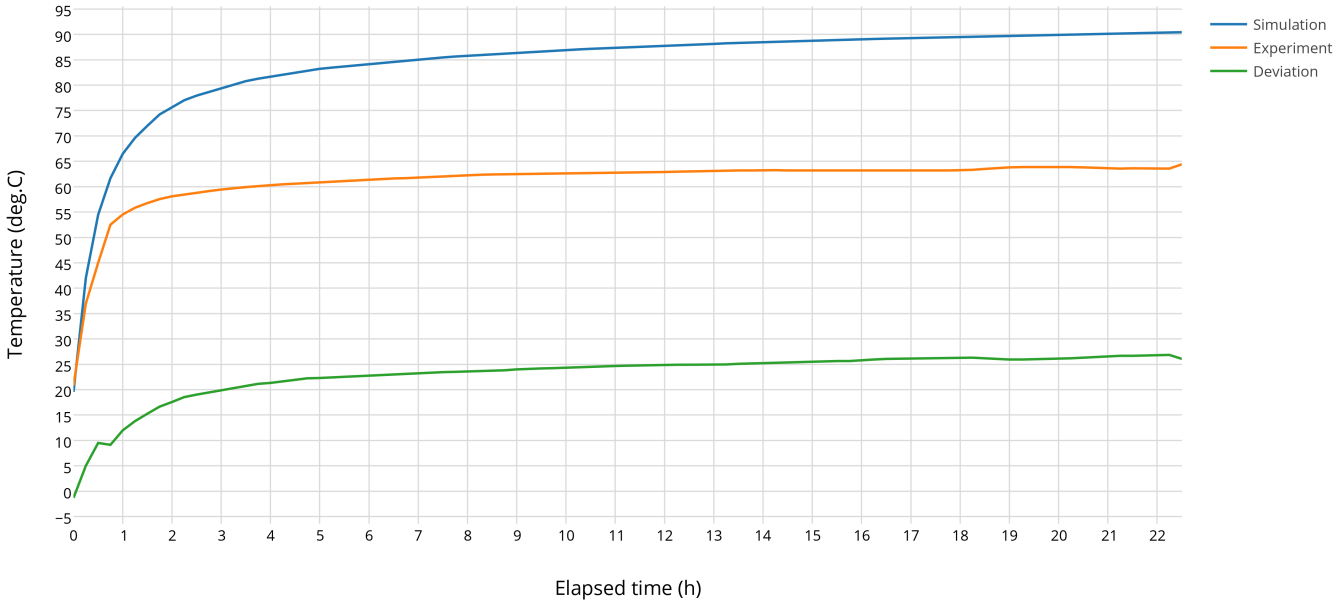

Figure 9.6: After adding the water, model 2.

9.4 Installation in Aluminum Pipe - Simulation Compared to Experiment

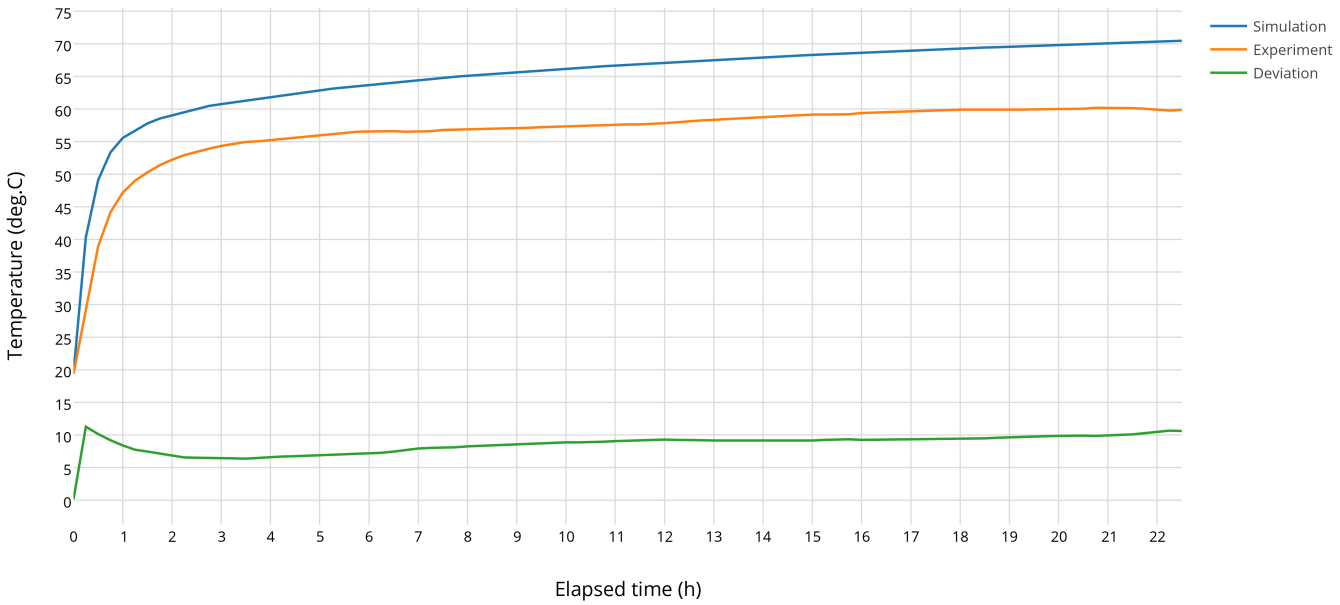

Figure 9.7: Before adding the water, model 3.

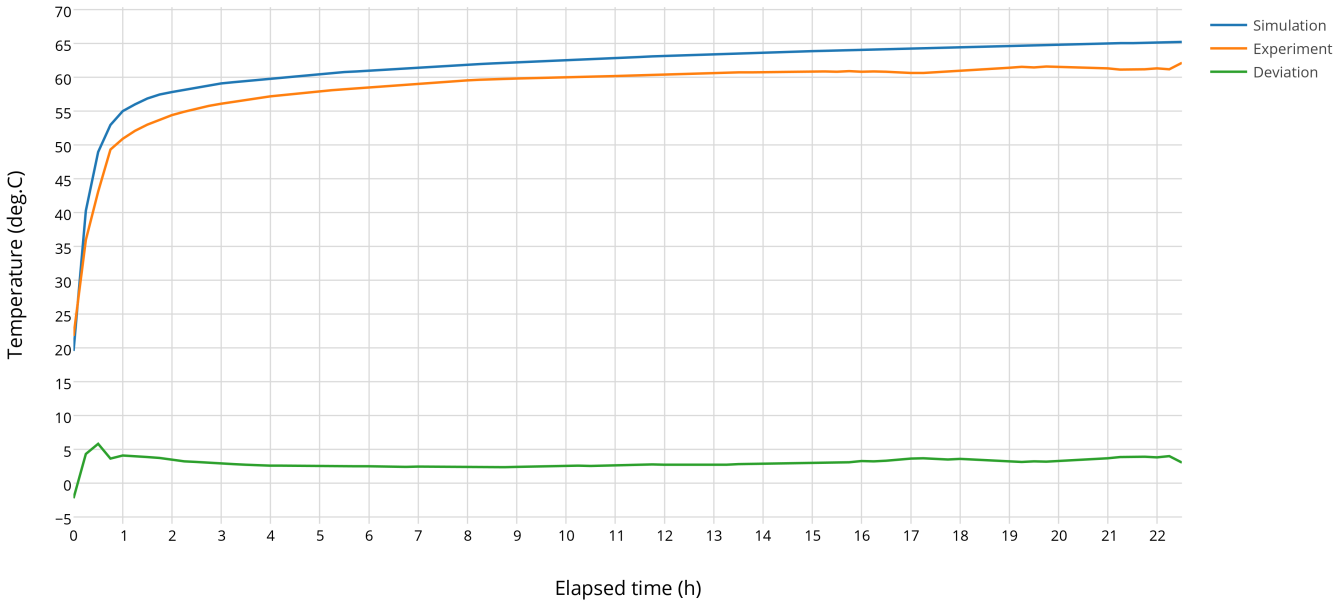

Figure 9.8: After adding the water, model 3.

Part III

Discussion

Chapter 10

Evaluation Of The Experiments

This part holds a discussion with emphasis on the results, and what the results implies based on the problem formulation. As a reminder, the problem formulation is as follows:

The primary goal of this work is to find out if a cable installed inside a buried aluminum pipe can increase the cables ampacity, when compared to a PVC pipe. The secondary goal is to assess the validity of the experiment by comparing the results to simulations in COMSOL, and to assess any observed deviations by the help of analytical procedures.

Throughout the upcoming discussion the models are designated with numbers, and the meaning of *model* is the physical models from the experiment. Each design is refereed to as:

- Direct laying in sand = **Model 1**
- PVC-pipe model = **Model 2**
- Aluminum-pipe model = **Model 3**

10.1 Observations From Experiment Part 1

The initial observation from figure 8.2, was that the temperature gradient between the models never stabilized. By studying the uppermost graphs, one can see a linear increase in temperature from model 1 to model 2, and visa versa. This indicates a transport of heat from model 2 towards model 1, which explains the increasing temperature gradient inside model 1 (between 0 and 1 meter in the graph). This means that the measured conductor temperature in model 1 was directly affected by the high temperature in the model 2. Parts of the heat from the conductors between model 1 and 2 also evacuated to the ambient surroundings. This fact probably limited the total heat transport from model 2 to model 1. These observations clearly indicates that the cables, hence the distance

between the models, were too short. With longer cables, the temperature gradients would have stabilized at some point, leading to negligible interference between the models. It has not been attempted to calculate how long these cables should have been to achieve this.

In addition, it was observed quite large temperature gradients internally in all models. As described in 6.4, the enter- and exit points of the pipes were filled with rockwool insulation. The objective of this action was to force heat in the radial direction, hence reduce the leakage of heat in the longitudinal direction, and rockwool seemed like a good idea to achieve that. To study the effect of the rockwool, some of it was removed from the aluminum pipe 3 hours into the experiment, leaving about 5 cm of rockwool inside the pipe openings. The effect can be seen from the green and red graph in figure 8.2, where a steep change in temperature (green line) occurs at the beginning and at the end of the aluminum pipe. The gradients between the center- and end of the pipe lowered after reducing the amount of rockwool (red line). It is reasonable to claim that a greater amount of heat left the model trough the pipe (z-direction) after removing some of the rockwool. Therefore, installation of rockwool or an equivalent material do pose an impact to the results. Further analysis on this problem is presented in section 10.4.
A final comment on the internal gradient, is that minor errors in readings from the thermocouple probes could have affected the results. This statement applies to all obtained results from the experiments. The extent of these errors, if they existed, are unknown.

The temperature between model 2 and 3 was in contrast to model 1, quite equal. This equality is by far not in correlation with the simulations in chapter 9, nor the results from the project thesis prior to this experiment [8]. As explained in section 8.2, it was suspected that the air gap between the cables and the bottom of the pipes had an impact on this situation. The principal and impact from this, is explained in the upcoming section.

10.1.1 Evaluation Of The Air Gap

One can assume that a gap between the conductors and the pipes increased $T\text{`}_4$, the *effective* thermal resistance of the air, even though the mass and volume of the air is equal, regardless of where the cable is placed in the pipe. In other words, the thermal resistance in the transition zone between the cables and the pipe increased. To illustrate the consequences, a similar scenario was simulated in COMSOL. The results are being presented in Figure 10.1 and 10.2. In Figure 10.2, the width of the gap was 3 mm. This distance was arbitrary chosen, since the real distance inside the pipes was inaccessible for measurements.

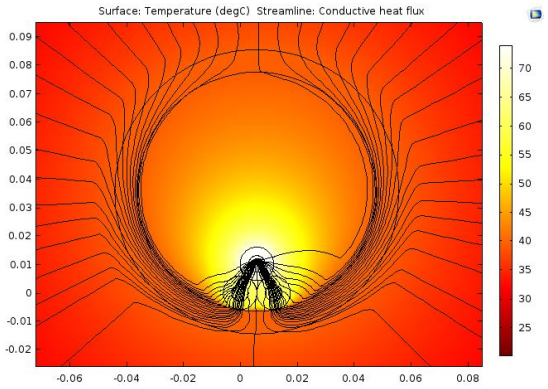

Figure 10.1: Direct contact.

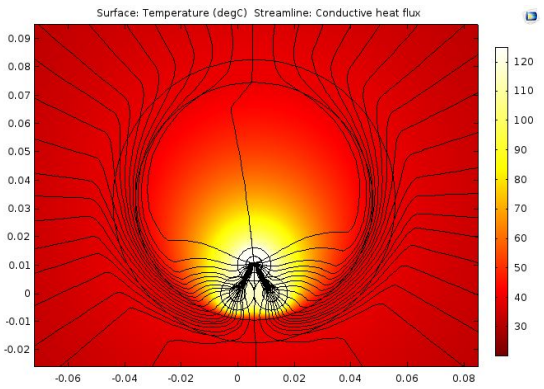

Figure 10.2: 3 mm separation.

In both simulations, a current of 82 A was applied until a steady state was reached, and with the exact same boundary conditions as in 5.1. The black lines represents the conductive heat flux, meaning the path in which heat flows. In figure 10.2, some of the heat lines seems to be forced into the air inside the pipe, whereas in figure 10.1 the majority of heat flows through the cables and into the pipe. As a result, the temperature increased to approximately 125 °C in contrast to 74 °C. This illustration clearly shows the impact of surrounding the conductors with air. One can therefore stress the importance of keeping the cables at the bottom, or in close contact with the pipes. However, if this is fulfilled in real life cable plants is a different question. One can assume that the cables will be somehow flat in the pipe at long, straight distances, especially if the cable is heavy (large cross section). This condition can probably change where the pipes are exposed to a change in direction (upwards, downwards and to the sides). In such situations, one can assume that the cable levitates and/or changes its position inside the pipe, for example to the center of the pipe. If this occurs, one can approximate a higher conductor temperature at that location. This should be taken into consideration when conducting FEM-analysis of tentative, future cable systems. This observation also shows the importance of conducting experiments to prove or disprove that the boundary conditions in COMSOL are accurate. For this example, these conditions were obviously quite inaccurate since the geometry of the cables were initially drawn in direct contact with the pipes.

10.2 Observations From Part 2

The action of increasing the contact surface seemed to have a positive effect regarding temperature. As figure 8.5 indicates, the temperature inside model 3 decreased with approximately 2.5 °C compared to model 2. The difference was not remarkable, but it did indicate an improvement in temperature performance which is in coherence with the simulations in figure 10.1 and 10.2.

The improvement can also be seen in the longitudinal conductor temperature. This was

presented in Figure 8.6, where the sets of temperatures were obtained at 5 different points in time. There are similarities between figure 8.1 and figure 8.6, but the development in temperature inside model 3 seemed more smooth and even after the improvement with wooden planks. This observation is quite interesting, considering that the cables were unevenly distributed inside the pipe, prior to installing the planks. The cables obviously had increased contact surface after the installation, and these two observations combined is an indication of a better heat transit from the conductors to the pipe. Simultaneously, the interpretation of this observation leads to a degree of ambiguity. If the planks itself held an even temperature distribution throughout the experiment, the conductor temperature could have been affected by that, regardless of the magnitude of the temperature. One must keep in mind that the thermocouple probes were installed straight under the surface of the insulation, and that the planks were on top of the insulation with quite high pressure due to a tight fit. However, no further examination was done to this observation, which somehow leads it to an element of uncertainty.
A different observation was that the temperature at 5.5 meters was higher at time = 1 hour, compared to the final temperature. A reasonable explanation for that, was the high current peak during the first half hour or so. The current peaked at $\approx$ 90 A (see figure 8.5), which gave a quite high transient heat production at the time. Why the temperature peaked at that location only, has not been examined.
Even though the temperature difference between model 2 and 3 increased during part 2, the difference was still very small compared to the simulations. It became suspected that the low thermal conductivity in the soil dominated the total thermal resistance, hence the fact that the thermal impact of the different pipes were not excelled in the results. Water was therefore added to the sand. The impact of this among other observations are discussed in the upcoming section.

10.3 Analytical Comparison Between Part 2 And 3

Part 3 of the experiment elapsed for 148 hours with many different applied currents. The primary objective of the long running time, was to seek for the impact of applying water to the sand. This impact was revealed by measuring the thermal conductivity in the sand. Sadly, the measurements resulted in ambiguity because of high differences between each measurement. It was therefore chosen to calculate the percentage distribution of thermal resistance in each model based on the obtained results from experiment part 2 and 3. The procedure is being presented in the upcoming subsection.

10.3.1 The Percentage Distribution Of Thermal Resistance In The Models

The following discussion contains a calculation and assessment of the percentage distribution of thermal resistance in the models, obtained from experiment 2 and 3. The amount of heat flowing in the radial direction experienced a total thermal resistance, seen from the conductors. This can be written as:

$$T_{toatal} = T_{insulation} + T_{air} + T_{pipe} + T_{sand} \tag{10.1}$$

For this experiment, the insulation of the conductors were only 3 mm thick, which means that the thermal resistance of the insulation can be neglected from this analysis. The aluminum pipe is also neglected, since the pipe was seen upon as a thermal short circuit. A final approximation is that each model contained an equal amount of sand. Therefore, T_{total} for the three models reduces to:

$$\begin{aligned} T_{model_1} &= T_{sand} \\ T_{model_2} &= T_{PVCpipe} + T_{air} + T_{sand} \\ T_{model_3} &= T_{air} + T_{sand} \end{aligned} \tag{10.2}$$

These are the total equivalent thermal resistances, which are located between the conductors and the ambient surroundings in model 1, 2 and 3. The temperature differences between the conductors an the surrounding air, $\Delta\Theta$, are known from part 2 of the experiment:

$$\begin{aligned} \Delta\Theta_{model_1} &= 36.7 - 20.0 = 16.7\,^{\circ}\mathrm{C} \\ \Delta\Theta_{model_2} &= 63.5 - 20.0 = 43.5\,^{\circ}\mathrm{C} \\ \Delta\Theta_{model_3} &= 61.3 - 20.0 = 41.3\,^{\circ}\mathrm{C} \end{aligned} \tag{10.3}$$

The ambient air temperature was approximately 20.0 °C during the whole experiment. The applied heat loss, P, from the cables and into the **radial direction of the models**, was approximated to be equal in all three models. This condition can be written as:

$$P_{model_1} = P_{model_2} = P_{model_3} \tag{10.4}$$

Which can be expanded to:

$$\frac{\Delta\Theta_{model_1}}{T_{model_1}} = \frac{\Delta\Theta_{model_2}}{T_{model_2}} = \frac{\Delta\Theta_{model_3}}{T_{model_3}} \tag{10.5}$$

The goal of aligning these equations, is to find the magnitude of each component of thermal resistance inside each model. By combining equation 10.5 and 10.2, one can find the following relation for the thermal resistance in the sand compared to the aluminum

pipe-model:

$$T_{model_1} = T_{sand} = \frac{\Delta\Theta_{model_1}}{\Delta\Theta_{model_3}} \cdot T_{model_3} = \frac{16.7}{41.3} \cdot T_{model_3} = 0.404 \cdot T_{model_3} \tag{10.6}$$

Which implies that the sand constituted of 40.4 %, and the air constituted the remaining 59.6 % of the total thermal resistance in the aluminum pipe-model (model 3). The same approach applies for the PVC-pipe model (model 2):

$$T_{model_1} = T_{sand} = \frac{\Delta\Theta_{model_1}}{\Delta\Theta_{model_2}} \cdot T_{model_2} = \frac{16.7}{43.5} \cdot T_{model_2} = 0.384 \cdot T_{model_2} \tag{10.7}$$

As suspected, the percentage share of thermal resistance in the sand decreased for model 2, compared to model 3. This is due to the PVC-pipe, since there were no other constructional differences between the models. To find the remaining share from the air and pipe, one must solve the following set of equations:

$$\begin{aligned} T_{model_2} &= T_{PVCpipe} + T_{air} + T_{sand} \\ T_{air} &= T_{model_3} - T_{sand} \\ \frac{\Delta\Theta_{model_3}}{T_{model_3}} &= \frac{\Delta\Theta_{model_2}}{T_{model_2}} \end{aligned} \tag{10.8}$$

The equations are solved with respect to $T_{PVCpipe}$:

$$T_{PVCpipe} = T_{model_2}(1 - \frac{\Delta\Theta_{model_3}}{\Delta\Theta_{model_2}}) = T_{model_2}(1 - \frac{41.3}{43.5}) = 0.05 \cdot T_{model_2} \tag{10.9}$$

This means that the PVC pipe was responsible for 5 % of the total radial thermal resistance in the model, leaving the final 56.6 % of the resistance to the air inside the pipe. To reveal the impact of adding water to the sand, **the exact same procedure was conducted for experiment 3.** The percentage distribution of thermal resistance in all 3 models are being visualised in Figure 10.3, both prior to, and after adding the water.

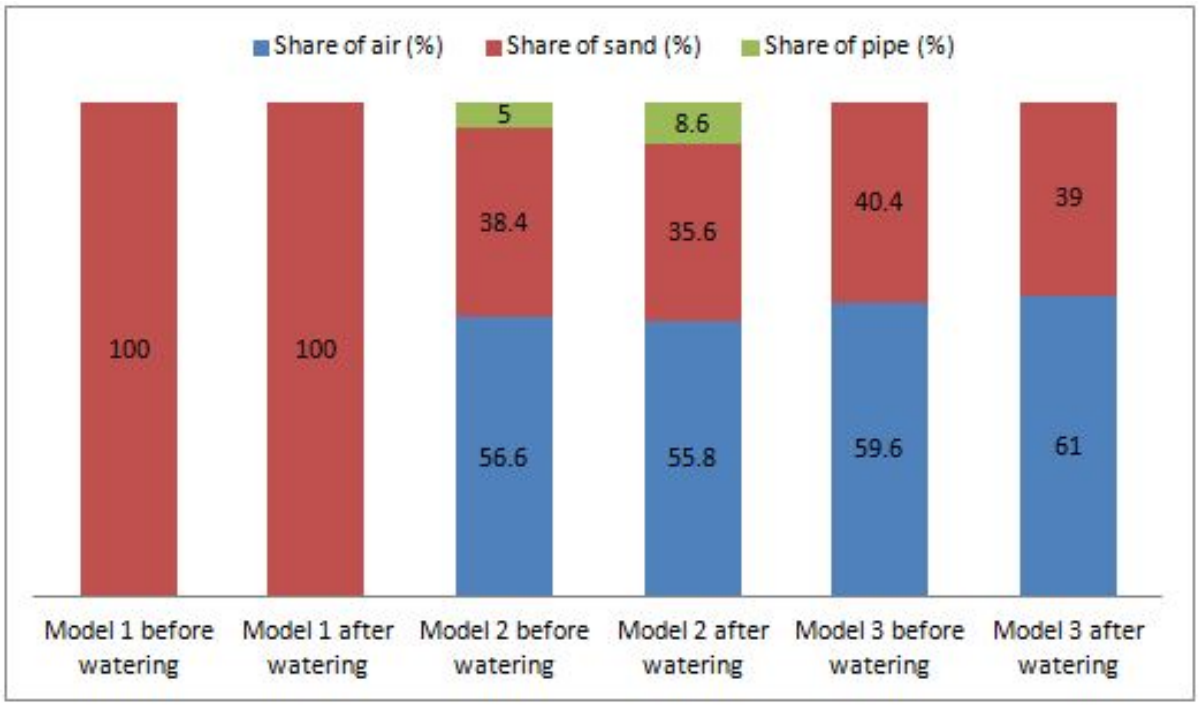

Figure 10.3: Percentage distribution of the thermal resistance in each model, referred to the radial direction away from the cables.

Figure 10.3 clearly shows that the air constitutes of more than 50 % of the total thermal resistance when a pipe is present, regardless of the pipe material. This clearly shows that the air itself has a significant impact to the ampacity of the cable due to the low thermal conductivity of air. On the contrary, by decreasing the thermal resistance in the soil (adding water), the percentage share from the pipe increased in model 2 from 5.0 to 8.6 %. These two observations initially means that the air inside the pipes dominates the thermal resistance, but that the PVC pipe makes a clear contribution to the total thermal resistance in the system. In addition, the conductor temperature inside model 3 was lower than for model 2. One can therefore conclude that the presence of an aluminum pipe compared to a PVC pipe can lower the operating temperature of the conductor, with the given constraints from the experiment. As a final notation, the percentage reduction in conductor temperature in model 3 compared to model 2 was according to table 8.1:

$$\frac{107.48 - 99.75}{107.48} \cdot 100\% = 7.19\% \tag{10.10}$$

When 115 A was applied and:

$$\frac{51.14 - 48.61}{51.14} \cdot 100\% = 4.95\% \tag{10.11}$$

When 65 A was applied. The reason for the relative deviation between the temperatures has not been examined, and is therefore an element of uncertainty.

10.4 Attempted Correction For Longitudinal Heat Loss

In chapter 9, simulations of two of the experiments were conducted. The main result was quite large deviations between the experiments and the simulations. The greatest deviation was found in model 2, where the simulation suggested a 45 °C higher conductor temperature compared to the experiment. As a plausible explanation for this, it was suspected that parts of the generated heat inside the models leaked out through the longitudinal direction instead of the radial direction. This so called leakage was not taken into account in the simulations, which could be a reason for higher simulated values compared to the experimental values. In this section, a *reduction factor* which represents this leakage was found. This factor was incorporated to COMSOL as an attempt to reduce the deviation between the primary simulations in chapter 9, and the obtained results from the experiment.

When conducting simulations in COMSOL, the programme solves the equations in 2 dimensions, x and y, whereas no heat flows in the z-direction. In other words, the z direction is treated as infinitely long, and no end effects are taken into account. In COMSOL, this means that all generated heat is transported in the radial direction, x and y, away from the heat source. The heat transport in COMSOL can therefore be expressed as:

$$3P_{gc} = P_{rc} \tag{10.12}$$

Where $3P_{gc}$ is the total generated heat in COMSOL, and P_{rc} is simply the heat transported in the radial direction. A thermal heat-flow equivalent of the COMSOL model can be expressed as in figure 10.4, where T_{rc} is the equivalent thermal resistance in the radial direction and Θ_{cc} and Θ_{ac} is the conductor- and ambient temperature, respectively.

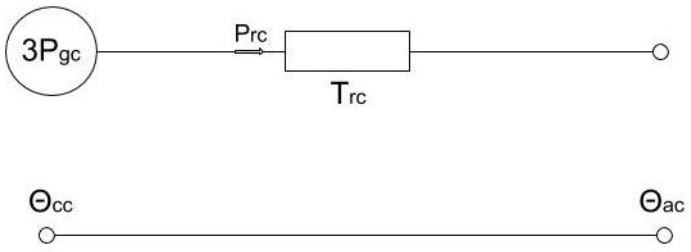

Figure 10.4: Thermal equivalent of the models in COMSOL

The longitudinal heat loss was suspected to leave the models through the conductors,

pipes and the walls of the models, where the last-mentioned was insulated with plates of styrofoam. Due to heat flow in both the radial *and* z-direction, the equation for heat flow in the models becomes:

$$3P_{ge} = P_{re} + P_{ze} \tag{10.13}$$

Where $3P_{ge}$ is the total generated heat from the experiment, whereas P_{re} and P_{ze} is the heat flow in the radial- and z-direction, respectively. The thermal equivalent for equation 10.13, hence the models, becomes:

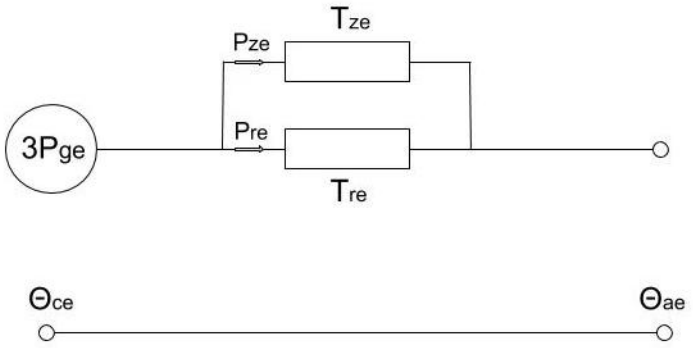

Figure 10.5: Thermal equivalent of the models in the experiment

Due to the paralell connection in figure 10.5, one can assume that the total thermal resistance in the physical models were lower than for the COMSOL models. If this is true, it can explain parts of the deviation between the simulation and the experiments, since a lower thermal resistance will give a lower temperature difference. To investigate if this could be a plausible explanation, one must start by identifying the magnitude of the heat loss in the z-direction, and thereafter subtract it from the applied heat in COMSOL. This is being explained by an example in the upcoming section.

10.4.1 Correction For Model 2

For this example, model 2 from experiment part 2 is used as a reference. As a first approximation, it is assumed that all heat loss in the z-direction for the PVC pipe went through the conductors. It is also assumed that the temperatures in all conductors were equal. Finally, it is assumed that the temperature gradient, $\frac{\partial \Theta_z}{\partial_l}$, was equal at both sides of the model. This means that the heat loss in both directions out/away from the model, was equal in magnitude. This is expressed as:

$$P_{ze} = 2 \cdot P_z \tag{10.14}$$

Where P_{ze} is the total heat loss, and P_z is the heat loss from one side of the model. Based on that, P_{ze} can be calculated in the following way:

$$P_{ze} = 2 \cdot P_z = 2 \cdot \frac{\Delta\Theta_z}{T_z} = 2 \cdot \frac{\Delta\Theta_z \cdot \sigma_{th}}{\Delta l/A} = 2 \cdot \frac{\partial\Theta_z}{\partial l} A \cdot \sigma_{th} \tag{10.15}$$

In which:

$\frac{\partial\Theta_z}{\partial l}$	is the temperature gradient at the boundary of the model
σ_{th}	is the thermal conductivity of aluminum (the conductor)
A	is the cross section of the conductor

The thermal probes were located 0.25 m from each other, with a difference of 12.1 °C. The thermal conductivity of aluminum is 238 (W/m·K) and the cross section of the conductor was 25 mm^2, so P_{ze} becomes:

$$P_{ze} = 2 \cdot \frac{\partial\Theta_z}{\partial l} A \cdot \sigma_{th} = 2 \cdot \frac{12.1}{0.25} \cdot 25 \cdot 10^{-6} \cdot 238 = 0.576W \tag{10.16}$$

And due to three conductors, the total heat loss in the z-direction becomes:

$$P_{ze,total} = 3P_{ze} = 1.72W \tag{10.17}$$

The purpose of calculating P_{ze} is to subtract it from the originally applied heat loss in COMSOL to compensate for the deviation between the simulated result, and the experimentally result. The way to do this in COMSOL, is by reducing the current in the conductors by the equivalent amount. Given that the original heat loss from 9 was P_{old}, the calculations for the new current becomes:

$$\begin{aligned} P_{new} &= P_{old} - P_{ze} \\ I_{new}^2 R &= I_{old}^2 R - P_{ze} \\ I_{new} &= \sqrt{\frac{I_{old}^2 R - P_{ze}}{R}} \\ &= \sqrt{\frac{82^2 \cdot 1.128 \cdot 10^{-3} - 0.576}{1.128 \cdot 10^{-3}}} \\ &= 78.82A \end{aligned} \tag{10.18}$$

The result of applying I_{new} compared to I_{old} is shown in Figure 10.6.

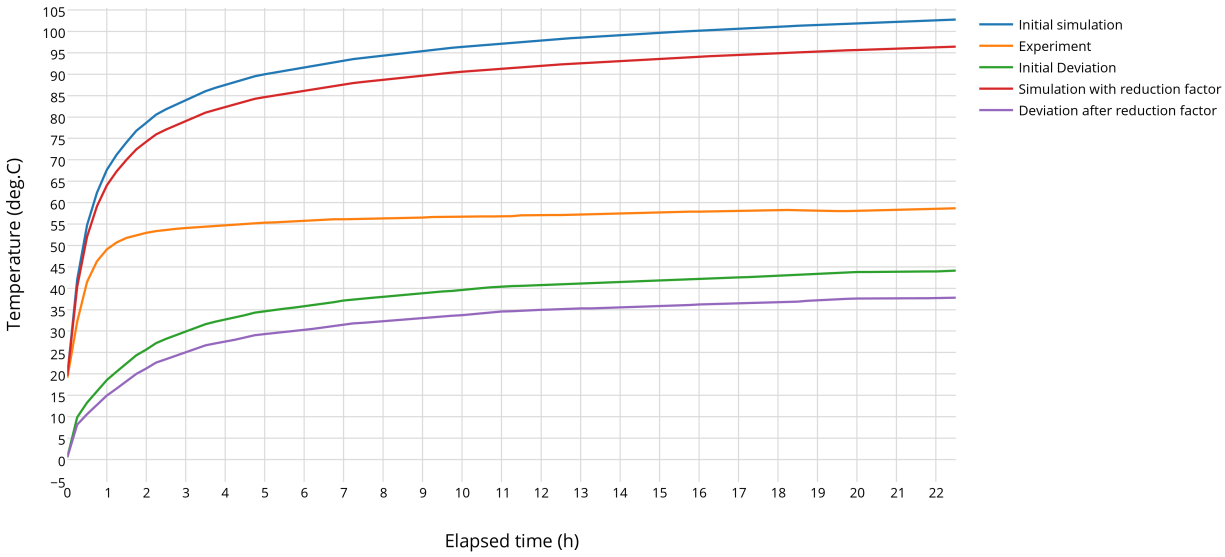

Figure 10.6: Simulated conductor temperatures in model 2, with and without the reduction factor P_{ze}.

Applying I_{new} obviously gave an improvement, where the deviation between the simulation and the experimental result decreased. As seen in Figure 10.6, the initial deviation was:

$$\frac{102.6 - 58.64}{102.6} 100\% = 42.84\% \tag{10.19}$$

After applying I_{new}, the new deviation is:

$$\frac{96.46 - 58.66}{96.46} 100\% = 39.18\% \tag{10.20}$$

However, a difference of 39.18% is still very much. This means that the calculated reduction factor P_{ze} for this example was insufficient. However, this example was based on the approximation that all heat loss in the z-direction occurred through the conductors. This is obviously incorrect.

A second approximation to the longitudinal heat loss, is that some of the heat evacuated through the rockwool (Glava). This can be calculated and added to P_{ze}, followed by a new simulation and hopefully an even better improvement compared to the original simulation in Figure 10.6. The procedure for calculating this, is the same as for calculating P_{ze} (equation 10.16). For this analysis, the presence of the wood inside the pipe is neglected.

As a start, one must know the temperature difference between the inner- an outer side of the rockwool. This was unfortunately not measured, except for the ambient temperature. Therefore, assumptions must be drawn. At time = 22.5 hours, the conductor temperature

was measured to 58.64 °C and the temperature at the top of the pipe was measured to 25.72 °C. The air temperature inside the pipe must therefore have been somewhere in between, so it is chosen to use 40 °C as a reference. The ambient temperature was 20 °C, giving $\Delta\Theta$ of 20 °C. The thickness of the installed rockwool was approximately 5 cm, and rockwool has a thermal conductivity of 0.035 (W/m·K)[9]. Finally, the effective area of the rockwool was simply the inner diameter of the pipe minus the area of the conductors:

$$A_{rocwool} = A_{pipe} - 3A_{conductor} = \pi r_i^2 - 3\pi r_c = \pi 0.049^2 - 3\pi(5.9 \cdot 10^{-}3)^2 = 0.00721m^2 \tag{10.21}$$

$$P_{rockwool} = 2 \cdot \frac{20}{0.05} \cdot 0.00721 \cdot 0.035 = 0.2W \tag{10.22}$$

$$P_{ze,new} = P_{ze} + P_{rockwool} \tag{10.23}$$

By replacing $P_{ze,new}$ with P_{ze} in equation 10.18, the calculated current becomes 77.69 A. By applying 77.69 A compared to 78.82 A into the COMSOL model, the final simulated conductor temperature becomes 94.28 °C compared to 96.46 °C. The new, total deviation between the simulated and experimental result becomes:

$$\frac{94.28 - 58.66}{94.28} 100\% = 37.78\% \tag{10.24}$$

In total, this means that reducing the applied heat loss in COMSOL by the calculated heat loss in the z-direction, had a marginal impact on the deviation between the experimental results, and the simulated results. The remained deviation of 37.78 % is therefore due to uncertainty elements of the experiment.

10.4.2 Correction For Model 3

To investigate heat-loss correction a step further, the exact same approach is used for the aluminum pipe. The conductor temperature was only measured at one side of the model, but it is assumed that the temperature was equal at both sides. The temperature gradient was approximately equal as for the PVC pipe. It is also assumed that the heat loss through the rockwool was the same as in the PVC pipe. In the previous subsection, the new current became 77.69 A. This current was applied to the COMSOL model of model 3, and the comparison between the simulations and the experimental result is being shown in Figure 10.7.

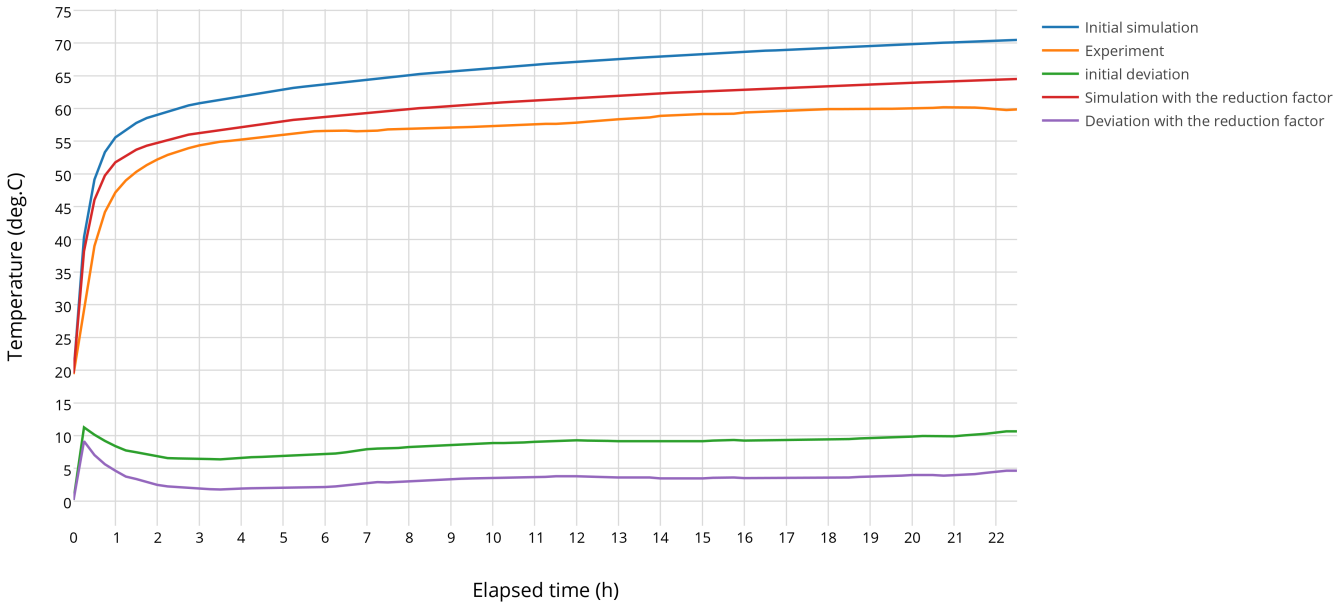

Figure 10.7: Simulated conductor temperatures inside the PVC pipe, with and without the reduction factor P_{ze}.

The deviation between the simulated- and experimental temperature was in the first place quite low. As seen in Figure 10.7, the deviation after including the reduction factor was even smaller. Before the reduction factor was included, the deviation was:

$$\frac{70.5 - 59.78}{70.5} 100\% = 15.2\% \tag{10.25}$$

And after:

$$\frac{64.49 - 59.78}{64.49} 100\% = 7.3\% \tag{10.26}$$

To sum up, the deviation after including the reduction factor was 37.78% for model 2, and 7.3% for model 3. This implies that for model 3, the simulations can be directly compared to the experiment with fairly high accuracy. This is, however, not the case for model 2, since the deviation was too high to neglect. One plausible explanation could be that the equivalent thermal resistance in the radial direction was higher for model 2 than first assumed. The total heat loss in both model 2 and 3 was equal, and more heat could have evacuated in the longitudinal direction in model 2 than first assumed, simply because of the higher radial thermal resistance in model 2 compared to model 3 (PVC versus aluminum). Regarding the extent of this discussion, there was not found any other plausible reasons or explanations to why this deviation was so large for model 2.

10.5 Loss in The Aluminum Pipe

The heat loss in the aluminum pipe in model 3 was both experimentally obtained (6.5.1), and simulated (9.1). The deviation between these two was enormous, since the experiment suggested a loss of 1.33 (W/m), and the simulation suggested 0.084 (W/m). One must keep in mind that the experiment contained elements of uncertainty. First, the time in which the loss was obtained elapsed to 300 seconds. During this time, some heat must have been transferred from the conductors to the pipe by conduction, radiation and convection. If so, most of this energy is assumed to have been conducted from the lowest conductors to the pipe, since they were in direct contact with each other. It is therefore plausible that the main temperature rise in the pipe was caused by external heat entering the pipe, and not by induced eddy currents, hence the heating process in the pipe was not adiabatic. As for the simulation, there is no reason to claim that FEM are inaccurate or untrustworthy regarding electric- and magnetic problems with given boundary conditions. As an example, the simulated heat loss in the conductors were 7.17 (W/m), and the calculated heat loss from the experiment per conductor is:

$$P_c = R_{AC} I^2 = 1.128 \cdot 10^{-3} \cdot 82^2 = 7.58(W/m) \tag{10.27}$$

There is a coherency between the simulation and the experiment regarding heat loss in the conductors, so the simulated induced heat loss in the pipe is assumed to be correct. In addition, the heat loss in the pipe was obtained over several currents (Figure 9.2), and no large losses were found. This finding supports that the simulated values are more reliable than the experimentally obtained values.

Based on the experiment, simulation and above discussion, the heat loss in the pipe are proven to be negligible when compared to the loss in the conductors. It is therefore not a disadvantage to use aluminum as a pipe material for cables, given that the parameters (loading, dimensions of the pipe and cable configuration) are equal.

Conclusion

This master thesis has emphasised whether an aluminum pipe can provide a better cooling of a power cable when compared to a traditional polymeric pipe under buried circumstances. It has also been paid attention to the experiment‘s validity by comparing it to FEM simulations.

The simulations suggested a higher conductor temperature than what was obtained in the experiments. This goes especially to the PVC-pipe model, where the temperature was 45 °C higher in the simulations. As an initial explanation, it was found that the models were too short, leading to significant leakage of heat in the longitudinal direction. The cable length between the models was also too short, leading to transport of heat through the cables from one model to the next. It was attempted to compensate for this leakage by the use of analytical approximations. This compensation gave improved accuracy between the simulations and the experiments, but not to a full extent. It was not attempted to fully reveal the reason for the remained deviations, which makes them elements of uncertainty. It is therefore concluded that models like the ones in this experiment must be longer to avoid errors due to end effects.

It was also revealed that the geometrical location of the cables inside the pipes affected the temperature. When the cables had a certain distance to the pipes, a higher temperature occurred compared to when the cables had good, physical contact with the pipes. The gap between the pipes and the cable occurred due to the stiffness and low weight of the cable, which is also a realistic scenario in practical cable installations. This reveals the importance of conducting experiments, since the boundary conditions in FEM does not automatically reflect the real situation. It is therefore important to be critical to these boundary conditions when applying FEM simulations in the planning phase of an underground cable grid.

The lowest operating conductor temperature in the experiments was observed in direct installation in sand, and the conductor temperatures were far higher inside both pipes. This observation is in coherence with the theory that air inside a pipe increases the thermal resistance in the system, thus a lower temperature will occur when a cable is

installed directly in sand. However, when comparing the performance of the two pipes in this experiment, the aluminum-pipe solution can be favoured for the following reasons:

- The operating conductor temperature was 4.95-7.19 % lower inside the aluminum pipe, compared to the PVC pipe, thus indicating a more efficient cooling caused by the aluminum pipe.
- The induced heat loss in the aluminum pipe was negligible when compared to the conductor loss.
- The aluminum pipe decreased the total thermal resistance in the system when compared to the PVC pipe.

Thus, aluminum pipes can be an initial reference for improved cooling of underground power cables when pipes are required as a design criteria. However, due to many elements of uncertainty, future investigations on this topic should be performed to fully reveal the potential of using aluminum pipes as a design of underground power cable systems. A suggestion is therefore being presented in the final, upcoming section of this thesis.

Recommendation For Future Work

It is recommended by the author to construct a full scale, 1:1 system of the same experiment as presented in this thesis. This should preferably be outdoors, with an excavation depth of 1 meter which is a typical solution in authentic cable plants. The cables should thereafter be installed in a PVC pipe, followed by an aluminum pipe with sufficient distance between the pipes. By doing this, end effects should be avoided. However, it is recommended to perform 2D axisymmetric simulations in COMSOL prior to constructing the experiment in order to determine the required length of the pipes, and the distance between the pipes. The cable must obviously be equipped with thermocouple probes to monitor the temperature. By doing all of this, one will obtain 100 % realistic results when compared to real life cable plants, and hopefully when compared to FEM simulations.

If the result favours the aluminum pipe compared to the PVC pipe, meaning a much lower temperature inside the aluminum pipe, one should expand the research further by optimizing the design of the aluminum pipe. As indicated, the aluminum pipe acts as a thermal short circuit in the first place. It also has a fairly high outer area, which is in direct contact with the soil. The authors hypothesis is that the heat transfer to the soil will increase further by applying heat sinks (cooling ribs) to the outer part of the pipe. This should effectively increase the outer area of the pipe, which is proportional to heat transfer, making the design even more efficient.

Bibliography

[1] George J. Anders *Rating of Electric Power Cables, Ampacity Computations for Transmission, Distribution and Industrial Applications* IEEE Press, 345 East 47th Street, New York, NY, IEEE ISBN 07803-1177-9, 1997.

[2] George J. Anders, Braun J.M, Vainberg M, Rizzetto S, Brakelmann, H. *Rating of Cables in a Nonuniform Thermal Environment* Toronto and Duisburg, IEEE 0-7803-5515-6, 1999.

[3] Barry Brusso, George J. Anders, C. Holyk *Power Cable Rating Equations - A Historical Perspective* IEEE Industry Application Magazine, July/August 2015.

[4] Nexans *60-500 kV High Voltage Underground Power Cables, XLPE Insulated Cables* `http://www.nexans.no/eservice/Norway-no_NO/fileLibrary/Download_540199654/Norway/files/Underground_power_cables.pdf`, 2015-12-10

[5] Hugh D. Young, Roger A. Freedman, A. Lewis Ford *Sears and Zemanskys's University Physics* Pearson, Addison-Wesley, 1301 Sansome Street, San Francisco, CA, ISBN 13: 978-0-321-76218-4, 2012

[6] Kyong Yong Lee, Jong Seok Yang, Yong Sung Choi, Dae Hee Park *Specific Heat and Thermal Conductivity Measurements of XLPE Insulator and Semiconductive Materials* School of Electrical, Electronic and Information Engineering Wonkwang University, Republic of Korea, IEEE 1-4244-0189-5, 2006

[7] M.S. Al-Saud, M.A. El-Kady, R.D. Findlay *Combined simulation–experimental approach to power cable thermal loading assessment* Department of Electrical and Computer Engineering, McMaster University, 1280, Main Street West, Hamilton, Ontario, Canada, L8S 4K1, 2008

[8] Beck Sletten, Tord *Calculation Of Transient Temperatures With Reference To Thermal Design Of Electric Power Cables* Department of Electric Power Engineering, Norwegian University of Science and Technology, 2015

[9] Glava AS, Data sheet 330, revision February 2012, url: http://media.glava.net/mediabank/store/7746/ProdDok-1665-1.pdf

[10] Wael Moutassem, George J. Anders *Calculation of the Eddy Current and Hysteresis Losses in Sheathed Cables Inside a Steel Pipe* IEEE TRANSACTIONS ON POWER DELIVERY, VOL. 25, NO. 4, OCTOBER 2010

[11] Prof. Dr. Ing. Robert Kristoffer Nilssen *Electromagnetics in Power Engineering* Department of Electrical Power Engineering, NTNU, TET 5100, Autumn 2012

[12] Bruce C. W. McGee, Fred E. Vermulen *Power Losses in Steel Pipe Delivering Very Large Currents* IEEE TRANSACTIONS ON POWER DELIVERY, Calgary, Alberta. Unknown year of publication.

[13] K Kawasaki, M Inami, T. Ishikawa *THEORETICAL CONSIDERATIONS ON EDDY CURRENT LOSSES IN NON-MAGNETIC AND MAGNETIC PIPIS FOR POWER TRANSMISSION SYSTEMS* IEEE Transactions on Power Apparatus and Systems, Vol. PAS-100, No. 2, Kawasaki, February 1981

[14] *COMSOL Multiphysics User's Guide* COMSOL 4.3a, November 2012

[15] IEC 60287-1-1 Edition 1.2 *Electric cables - Calculation of the current rating - Part 1-1: Current rating equations (100 % load factor) and calculations of losses - General* ©IEC, Geneva, Switzerland